Blow-up in reaction-diffusion systems

Sewalt, L.

Lotte Sewalt

Blow-up in reaction-diffusion systems

Bachelor Thesis, June 2010

Supervisor: dr. V. Rottschäfer

Leiden University

Abstract
In 2003 Arjen Doelman and Tasso J. Kaper published an article named *Semistrong Pulse Interactions in a Class of Coupled Reaction-Diffusion Equations.* In this article blow-up behavior was found in simulations of two modified Gierer-Meinhardt systems. In this thesis this behavior in both of these systems is analyzed. First we will use rescalings to construct explicit first order expressions for the blow-up solutions. These theoretical results are illustrated by simulations.

Contents

1 Introduction

1.1 Reaction-diffusion system

In this thesis we will study blow-up behavior of the solutions in the following class of dynamical systems:

$$(1) \qquad \begin{cases} \varepsilon^2 U_t &= U_{xx} - \varepsilon^2 \mu U + f(U)V^2, \\ V_t &= \varepsilon^2 V_{xx} - V + g(U)V^2. \end{cases}$$

U and V are positive functions defined for $(x,t) \in \mathbb{R} \times \mathbb{R}^+$, $\mu > 0$ is a parameter, $0 < \varepsilon \ll 1$ and f and g are smooth positive functions on $U > 0$ which may have mild singularities at $U = 0$. Because U and V depend on both x and t, and derivatives with respect to both of these variables are included in the equations, they are called partial differential equations.

A system like this is called a coupled reaction-diffusion system in two components. Reaction-diffusion systems describe the behavior and interactions of two or more types of particles. The U_{xx} and V_{xx} terms are the diffusion terms and they describe the spread of these particles. The reaction terms are represented by $f(U)$ and $g(U)$ and these terms describe in what way the particles interact with one another. Both U and V occur in both equations, therefore, they depend on each other. Thus, in general, the system cannot be written into two separate equations. The above system (1) contains a large class of reaction-diffusion systems. The so-called Gierer-Meinhardt and Gray-Scott models are included in the above class of equations. Both these models describe the behavior of chemical species under certain circumstances.

1.2 The Gierer-Meinhardt model

As mentioned above, the Gierer-Meinhardt equations are included in the class of reaction-diffusion systems (1). This model was formulated by Alfred Gierer and Hans Meinhardt in 1972, see [4]. It describes the morphogenesis of organisms, and the pattern formation of tissue in particular. The central question is: if all cells of an organism start out the same, how can it be that they could grow out so differently? Sometimes, starting from almost homogeneous tissue, spatial patterns and different structures are formed, and these patterns could be independent of the total size of the tissue.

In 1952, Alan Turing already published a paper on morphogenesis which described on how patterned morphogen distribution could result from auto- and cross catalysis. A chemical reaction is called *autocatalytic* or *self-enhancing* if the reaction product is itself the catalyst for that reaction. A set of two chemical reactions is called cross-catalytic if the two reactions work as a catalyst for each other. Gierer and Meinhardt used Turing's conclusions to describe biological pattern formation more thoroughly. They constructed a model consisting of two partial differential equations of reaction-diffusion type. It describes the concentrations of two substances, a self-enhancing activator and an inhibitor. The system is therefore called an activator-inhibitor system. The activator is so-called short-range autocatalytic.

An example of short-range activation, is that when part of a healthy organ of person A is transplanted into the body of person B, it could start to grow up to regular size in the bodies of both A and B. It is obvious that self-enhancement alone would lead to unlimited increase of the activator. Therefore the activator usually

produces its own antagonist, which is a long-range inhibitor. The inhibiting action of an organ on the formation of a new similar organ that was transplanted close to the former one, could be attributed to long-range inhibition. A lot of aspects of morphogenesis can be explained in terms of activators and inhibitors. Gierer and Meinhardt included various kinds of activator-inhibitor models in their paper, see [4] and [5].

An example of a (simplified version of the) model that Gierer and Meinhardt found for the activator a and inhibitor h is:

$$\left\{ \begin{array}{rcl} \frac{\partial a}{\partial t} & = & D_a \triangle a + \rho_a \left(\frac{a^2}{h} - a \right), \\ \frac{\partial h}{\partial t} & = & D_h \triangle h + \rho_h \left(a^2 - h \right). \end{array} \right. \tag{2}$$

Here $\triangle$ is the Laplace operator which depends on the space-dimension. In a two-dimensional system $\triangle = \partial^2/\partial x^2 + \partial^2/\partial y^2$. Here D_a and D_h are the diffusion rates of the activator a and inhibitor h respectively and ρ_a and ρ_h are the corresponding cross-reaction coefficients. To prevent activator from infinite growth the inhibitor should slow down the increase of a. This means that the diffusion of h should be faster than the diffusion of a, i.e. $D_h \gg D_a$. Furthermore, convenient length and time units can be found in which $\rho_a = D_h = 1$, which reduces the number of parameters. The reaction term $\rho_h(a^2 - h)$ can be explained as two particles a react with one particle h. For further explanation, see [5].

Another system that was obtained in [4] is an activator-substrate system. This is based on another way to stop the growth of the activator. The inhibitions could also be achieved by the depletion of a substance s that is required for the autocatalysis. In this case, the system is called an activator-substrate system. In its simplest form it looks like:

$$\begin{array}{rcl} \frac{\partial a}{\partial t} & = & D_a \triangle a + \rho_a \left(a^2 s - a \right), \\ \frac{\partial s}{\partial t} & = & D_s \triangle s + \rho_s \left(1 - a^2 s \right). \end{array}$$

The parameters have the same meaning as in (2). Here s is supposed to be the antagonist. Again, the inhibition caused by the substrate is only effective if $D_s \gg D_a$.

1.3 Applications of the Gierer-Meinhardt model

In biological structures, polygonal patterns are very common. Think about a giraffe's coat or the veins in the wings of a dragonfly.

Figure 1: Polygonal patterns: Giraffe skin

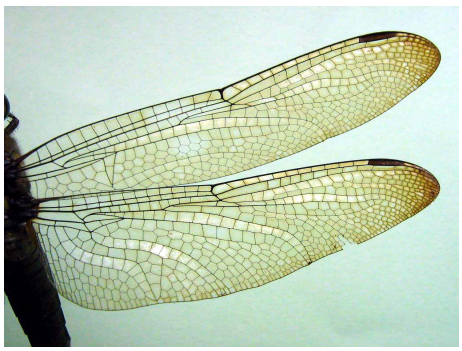

Figure 2: Polygonal patterns: Veins in wings of a dragonfly

The main difference between the morphogenesis of the coat of a giraffe and the veins in the wings of a dragonfly, is that the patterns on a giraffe, once formed, does not change. This is not the case for the dragonfly. The veins in its wings are not produced in a single step at a particular moment of the development. Therefore, the models that describe the formation of both these patterns are different.

For the dragonfly, it is assumed that at an early stage of its development, a simple pattern is laid down. The main veins are already formed, but the smaller branches are developed later, in order to strengthen the growing wings. The model describing this behavior is a combination of an activator-substrate at first, which should then be replaced by an activator-inhibitor model. The first model (activator-substrate) is given by:

$$\begin{aligned} \frac{\partial a}{\partial t} &= D_a \triangle a + \rho_a \left(\frac{a^2 s}{1 + \kappa_a b^2} - a \right) + \sigma_a, \\ \frac{\partial s}{\partial t} &= D_s \triangle s - \rho_s \left(\frac{a^2 s}{1 + \kappa_a b^2} \right) + \sigma_s. \end{aligned}$$

This describes how a pattern of activation mounds is produced. In terms of the dragonfly, it desnotes how the main veins are formed. This first pattern triggers another system, which is an activator-inhibitor system:

$$\begin{aligned} \frac{\partial b}{\partial t} &= D_b \triangle b + \rho_b \left(\frac{s^2}{1 + \kappa_b a b^2} \left(\frac{b^2}{h} - \sigma_b \right) - b \right), \\ \frac{\partial h}{\partial t} &= D_h \triangle h - \rho_h \left(b^2 - h \right). \end{aligned}$$

In this system, the concentration of a determines the saturation value of the activator b. When a has a high concentration, the (b, h) system is turned off. At that moment, b has a low concentration. On the other hand, when a had a low concentration, the (b, h) system is triggered and it will form a pattern. This formation is enhanced by s, the substrate, because of the square term in the first equation of the second system. This will have most impact when s is big, and when the concentration of the substrate is high, the concentration of a must be low. Therefore,

the concentration of b is the highest in regions that are most distant from maxima of a. The action of h ensures that the stripelike patterns b forms, become sharp. See figure 3.

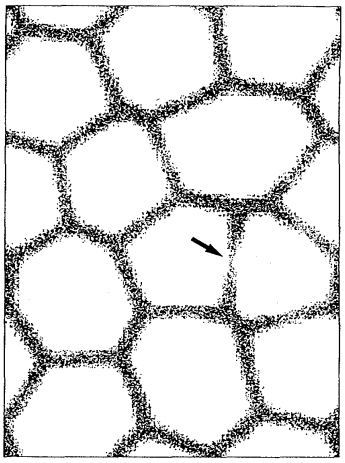

Figure 3: Simulation of [5] based on the system described above. The density of the dots is proportional to the concentration of b. The arrow points at the completion of a boundary between two domains.

It turns out that this model works very well in describing patterns. In general, activator-inhibitor and activator-substrate systems are used to describe the formation of biological patterns.

1.4 From Gierer-Meinhardt to blow-up

When in system (1), $f(U)$ is chosen a constant f, and $g(U) = 1/U$, the system is an activator-inhibitor system. This can be seen as follows when comparing system (1) to (2). In (1), there is only one space variable, so $\triangle = \partial^2/\partial x^2$. When $\rho_a = 1$ and $D_a = \varepsilon^2$, the V in (1) plays the role of the activator a in (2). Setting, in addition, $D_h = \varepsilon^{-2}$ and $\mu = \rho_h = f/\varepsilon^2$, U plays the role of the inhibitor h. Therefore system (1) is with these choices an activator-inhibitor system, and the Gierer-Meinhardt model is included in the class of systems described by (1). The model (1) was analyzed in [3]. In this article, the authors analyzed the interactions of two-pulse solutions of this system. Certain simulations they performed look like figure 4. We would like to thank A. Doelman and T.J. Kaper for letting us use these figures.

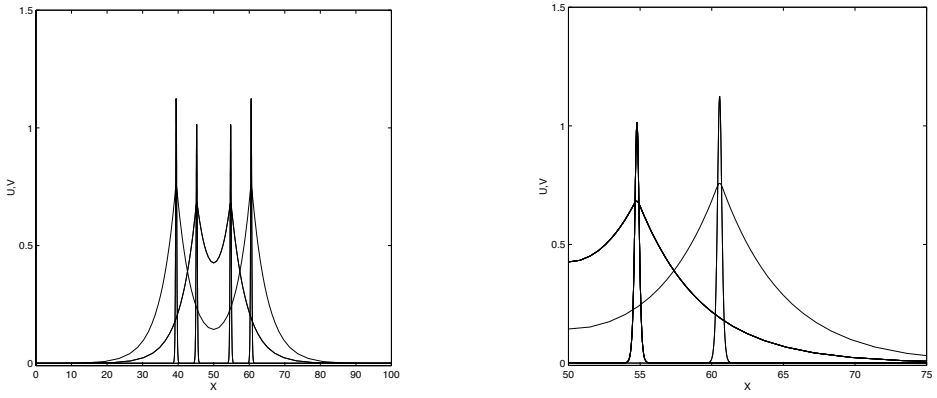

Figure 4: On the left: A two-pulse solution obtained from numerical simulations of [3] with $f(U) = 1$ and $g(U) = 1/U$, for $\varepsilon^2 = 0.01$ and $\mu = 5$ at two instants of time. The pulses repel each other. On the right a magnification. he narrow, high peak is the simulation of V, the activator, and the other peak is U, the inhibitor.

In particular, the authors of [3] did some simulations with two modified Gierer-Meinhardt systems, namely where $f(U) = 1$ and either $g(U) = 1/U + a$ or $g(U) = (1/U) + (b/\sqrt{U})$, with a and b positive constants. The classical Gierer-Meinhardt case appears when a or b is equal to zero.
When $a = 0.342$, $\mu = 5$ and $\varepsilon^2 = 0.01$, finite-time blow-up occurs in the simulations. This means that the solutions blow up to infinity in finite time.

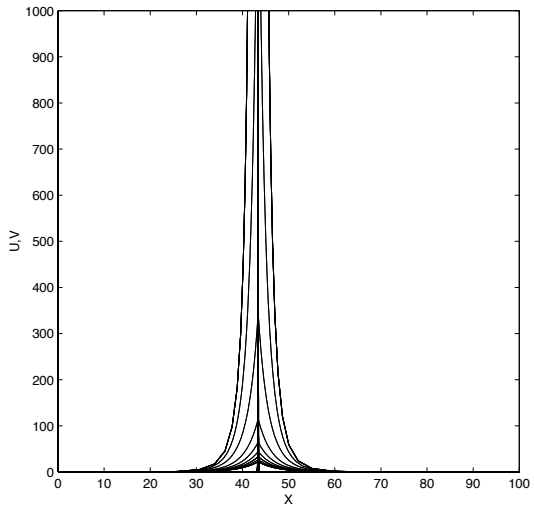

Figure 5: Simulation of [3] of the modified Gierer-Meinhardt equation with $g(U) = 1/U + a$, and $\mu = 5$,$\varepsilon^2 = 0.01$, and $a = 0.342$. The simulations for $t = 57.8, 57.9, 58.0, 58.1, 58.1, 58.2, 58.3, 58.4, 58.45, 48.47$ are presented. In the simulations U and V blow up at $t \approx 58.472$.

This is of course very strange behavior in a system that describes a biological process. It could be a reason to question the correctness of the model. Apparently it is not totally fitting. Of course, it is possible that choosing the parameters this way never occurs in the biological processes that the models describe. Often models are derived assuming that the quantities remain $\mathcal{O}(1)$. Then blow-up suggests that another model should be used.
This finite time blow-up behavior therefore needs some further examination and in the next few chapters we will do this. We will take a closer look at simulations of the system, and solutions fitting to these simulations.

2 First analysis of the system

First we will try to analyze the solutions of (1) for the Gierer-Meinhardt and the two modified Gierer-Meinhardt cases. This was done in [3] as well. Consider:

$$\left\{ \begin{array}{lcl} \varepsilon^2 U_t &=& U_{xx} - \varepsilon^2 \mu U + V^2, \\ V_t &=& \varepsilon^2 V_{xx} - V + g(U)V^2, \end{array} \right. \tag{3}$$

where either $g(U) = 1/U$ for the classical Gierer-Meinhardt equation, or $g(U) = 1/U + a$ or $g(U) = (1/U) + (b/\sqrt{U})$ for the modified Gierer-Meinhardt case.
We would like to construct stationary solutions that look like figure 4. Therefore we can assume that $U(x,t) = u(x)$, and $V(x,t) = v(x)$. Because U and V behave very differently near the pulse than far from it, we will consider two scalings of the x-variable.

$$\chi = \varepsilon x,$$
$$z = \frac{x}{\varepsilon}.$$

Here the χ-scale is a wide range x-variable and is called the slow variable, for values of x that are far from the pulse, and z works as an x-variable to zoom in close to the pulse and is called the fast variable. When x is of $\mathcal{O}(\varepsilon)$, z is $\mathcal{O}(1)$, and when x is of $\mathcal{O}(\frac{1}{\varepsilon})$, χ is of $\mathcal{O}(1)$. We will consider the χ-level first, $u_{xx} = \varepsilon^2 u_{\chi\chi}$ and $v_{xx} = \varepsilon^2 v_{\chi\chi}$. The system becomes:

$$\left\{ \begin{array}{lcl} 0 &=& \varepsilon^2(u_{\chi\chi} - \mu u) + v^2, \\ 0 &=& \varepsilon^4 v_{\chi\chi} - v + g(u)v^2. \end{array} \right. \tag{4}$$

This system of two second order ODE's can be written as a system of four first order ODE's. There are several ways of doing this, for example:

$$\begin{array}{lcl} \varepsilon u' &=& p; \\ \varepsilon p' &=& \varepsilon^2 \mu u - v^2; \\ \varepsilon^2 v' &=& q; \\ \varepsilon^2 q' &=& v - g(u)v^2, \end{array} \tag{5}$$

which is called the slow system. When we consider the equations at the different levels of ε, for $\mathcal{O}(1)$ the first two equations of system (5) become:

$$\begin{array}{lcl} 0 &=& p, \\ 0 &=& -v^2. \end{array}$$

This means that $v \equiv 0$. In figure 4 we see that it is indeed the case that far from the pulse, the V solution is equal to zero. For the first equation of (4), this means that, at the $\mathcal{O}(\varepsilon^2)$ level:

$$0 = u'' - \mu u.$$

This equation has solutions of the form

$$u = c_1 e^{\sqrt{\mu}\chi} + c_2 e^{-\sqrt{\mu}\chi},$$

where c_1 and c_2 are constants. As we could see in figure 4, it is indeed the case that far from the pulse, u behaves like an exponential function. To match the solution perfectly, we would like:

$$\lim_{\chi \to \pm\infty} u(\chi) = 0.$$

Since we only looked at the wide range scale χ, this means that:

$$\begin{array}{rcll} u & \sim & e^{\sqrt{\mu}\chi} & \text{for } \chi \in (-\infty, -\varepsilon), \\ u & \sim & e^{-\sqrt{\mu}\chi} & \text{for } \chi \in (\varepsilon, \infty). \end{array}$$

For now, it is not determined what the behavior of u is for $\chi \in (-\varepsilon, \varepsilon)$, because we constructed this solution up to leading order.
Therefore, we will now take a look at the fast variable scale, because when $\chi \in (-\varepsilon, \varepsilon)$, this means that $z \in (-\frac{1}{\varepsilon}, \frac{1}{\varepsilon})$. For small ε, this equal a large part of $\mathbb{R}$.

Now we will take a look at the system at fast variable level. Stationary solutions satisfy:

$$\left\{ \begin{array}{rcl} 0 & = & \frac{1}{\varepsilon^2} u_{zz} - \varepsilon^2 \mu u + v^2, \\ 0 & = & v_{zz} - v + g(u) v^2. \end{array} \right. \tag{6}$$

Again, these two second order ODE's can be split up into four first order ODE's:

$$\begin{array}{rcl} u' & = & \varepsilon p, \\ p' & = & -\varepsilon v^2 + \varepsilon^3 \mu u, \\ v' & = & q, \\ q' & = & v - g(u) v^2, \end{array} \tag{7}$$

which is called the fast system. There are more ways to write the second order equations into two first order equations, but these expressions will later on turn out to be more convenient than other rewritings.

Looking at the first two equations of (7), we find that because $0 < \varepsilon \ll 1$, up to first order of ε, the equations become:

$$u' = 0,$$

$$p' = 0.$$

This means that u is constant, say $u \equiv u_0$. This means that near the pulse, where V gets very high and steep, U is approximately constant. Indeed, in figure 4, we can see that where V has its pulse, U is already very large and near its maximum. In the last two equations of (7) all ε's are scaled out, so the entire equations are of first order.

$$v'' = v - g(u) v^2.$$

But since u is constant u_0 for the fast variable up till leading orders, this equation is no longer depends on u:

$$v'' = v - g(u_0) v^2.$$

This is a solvable equation for v, because $g(u_0)$ is now just a constant. The solution of this ODE for $v(z)$ is :

$$v(z) = \frac{3}{2g(u_0)} \operatorname{sech}^2 \left(\frac{z}{2} \right)$$

When $g(u_0) = 1$, this solution looks like figure 6.

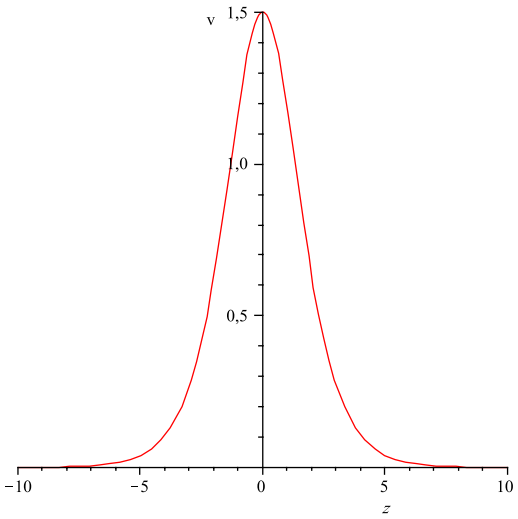

Figure 6: A plot of $v(z)$ for $g(u_0) = 1$.

Remember that this is the behavior of v zoomed in on x, it is the solution for the narrow range x-variable z. So this would be the behavior of v very close to the pulse, and as we can see in figure 7, it actually has the form of a pulse, and the solution is very close to zero for large z-values.

$$\begin{aligned}
\lim_{z\to\infty} v(z) &= \lim_{z\to\infty} \frac{3}{2g(u_0)} \operatorname{sech}^2\left(\frac{z}{2}\right) \\
&= \frac{3}{2g(u_0)} \lim_{z\to\infty} \operatorname{sech}^2\left(\frac{z}{2}\right) \\
&= \frac{3}{2g(u_0)} \lim_{z\to\infty} \frac{1}{\left(\frac{1}{2}\left(e^{\frac{z}{2}} + e^{-\frac{z}{2}}\right)\right)^2} \\
&= \frac{3}{2g(u_0)} \frac{1}{\left(\frac{1}{2}\left(\lim_{z\to\infty} e^{\frac{z}{2}} + e^{-\frac{z}{2}}\right)\right)^2} \\
&= \frac{3}{2g(u_0)} \frac{1}{\left(\frac{1}{2}\left(\lim_{z\to\infty} e^{\frac{z}{2}}\right)\right)^2} \\
&= \frac{3}{2g(u_0)} 4 \left(\lim_{z\to\infty} e^{-\frac{z}{2}}\right)^{-2} \\
&= \frac{3}{2g(u_0)} 4 \left(0\right)^{-2} \\
&= 0
\end{aligned}$$

Since the solution for v is symmetric, it has the same limit as $z \to -\infty$. Therefore, the two solutions found for v, at the z- and χ-scale, can be matched together to yield a new solution that fits exactly with figure 4.
Now let's glue the two solutions for u together. We know now that u is constant for $z \in (-\frac{1}{\varepsilon}, \frac{1}{\varepsilon})$, so for $\chi \in (-\varepsilon, \varepsilon)$.

$$\begin{aligned}
u &\sim c_1 e^{\sqrt{\mu}\chi} && \text{for } \chi \in (-\infty, -\varepsilon), \\
u &\sim u_0 && \text{for } \chi \in (-\varepsilon, \varepsilon), \\
u &\sim c_2 e^{-\sqrt{\mu}\chi} && \text{for } \chi \in (\varepsilon, \infty).
\end{aligned}$$

So we find:

$$\begin{aligned}
u(\chi = -\varepsilon) &\approx u(0) = c_1, \\
u(\chi = \varepsilon) &\approx u(0) = c_2.
\end{aligned}$$

Therefore $c_1 = c_2$, and to match this solution with the constant solution $u = u_0$ at $(-\varepsilon, \varepsilon)$, we find $c_1 = c_2 = u_0$.
Now we need to find this constant. Another method is imposed to find it. We constructed u in a way that makes it continuous, but one should notice that its derivative is not continuous. It makes a jump in the interval $\chi \in (-\varepsilon, \varepsilon)$.
This jump, Δu_χ can be determined, by defining it in a clever way.

$$\Delta u_\chi = \int_{-\varepsilon}^{\varepsilon} u_{\chi\chi} d\chi = \frac{1}{\varepsilon^2} \int_{-\frac{1}{\varepsilon}}^{\frac{1}{\varepsilon}} u_{zz} dz \approx \frac{1}{\varepsilon^2} \int_{-\infty}^{\infty} u_{zz} dz$$

The last approximation is legitimate because ε is very small and we will look at lower order terms only.
We know from (10) that $u_{zz} = \varepsilon^4 \mu u - \varepsilon^2 v^2 = -\varepsilon^2 v^2 + \mathcal{O}(\varepsilon^4)$, and that on the z-scale, $v = \frac{3}{2g(u_0)} \text{sech}^2\left(\frac{z}{2}\right)$.

$$\begin{aligned}
\Delta u_\chi &\approx \frac{1}{\varepsilon^2} \int_{-\infty}^{\infty} -\varepsilon^2 v^2 dz + \mathcal{O}(\varepsilon^4) \\
&= \frac{1}{\varepsilon^2} \int_{-\infty}^{\infty} -\varepsilon^2 \left(\frac{3}{2g(u_0)} \text{sech}^2\left(\frac{z}{2}\right) \right) dz + \mathcal{O}(\varepsilon^4) \\
&= \int_{-\infty}^{\infty} \frac{3}{2g(u_0)} \text{sech}^2\left(\frac{z}{2}\right) dz + \mathcal{O}(\varepsilon^4) \\
&= -\frac{6}{(g(u_0))^2}
\end{aligned}$$

We can also evaluate u_χ at $-\varepsilon$ and ε another way, since we know that $u = c_1 e^{\sqrt{\mu}\chi} = u_0 e^{\sqrt{\mu}\chi}$ for $\chi \in (-\infty, -\varepsilon)$, and $u = c_2 e^{-\sqrt{\mu}\chi} = u_0 e^{-\sqrt{\mu}\chi}$ for $\chi \in (\varepsilon, \infty)$

$$\begin{aligned}
\left.\frac{d}{dx} u\right|_{\chi=-\varepsilon} &= \left. \sqrt{\mu} u_0 e^{\sqrt{\mu}\chi} \right|_{\chi=-\varepsilon} \\
&= \sqrt{\mu} u_0 \text{ (up to leading order)} \\
\left.\frac{d}{dx} u\right|_{\chi=\varepsilon} &= \left. -\sqrt{\mu} u_0 e^{-\sqrt{\mu}\chi} \right|_{\chi=\varepsilon} \\
&= -\sqrt{\mu} u_0 \text{ (up to leading order)}
\end{aligned}$$

But we know that Δu_χ in $\chi \in (-\varepsilon, \varepsilon)$ is equal to $-\frac{6}{(g(u_0))^2}$. So:

$$-\sqrt{\mu} u_0 - \sqrt{\mu} u_0 = -\frac{6}{(g(u_0))^2}$$

Which gives us u_0:

$$u_0 = \frac{1}{2\sqrt{\mu}} \frac{6}{(g(u_0))^2} = \frac{3}{(g(u_0))^2 \sqrt{\mu}}$$

3 Blow-up rescaling

The difficulty in studying blow-up lies in the fact that blow-up solutions are not bounded. Therefore we rescale out the blow-up behavior. Since the blow-up occurs at a certain moment in time we assume that the solutions can be split into two bounded solutions. When a bounded solution is divided by a solution that becomes zero at a certain point, this will lead to infinity. Therefore, when a solution $V(x,t)$ blows up in finite time, we can assume that:

$$V(x,t) = \frac{w(x,t)}{L(t)},$$

where $L(t) \to 0$ as t approaches the blow-up time T. There are of course many functions L that satisfy this condition.

The rescaling should not alter the differential equations, therefore the two variables on which V and U depend, should be rescaled as well. There are various ways for this rescaling. The three that are discussed in this chapter are the ones used in this thesis. After rescaling, the differential equations can be rewritten into a new pair of PDE's of two new bounded functions depending on two new variables. This way, the blow-up behavior is scaled out and the new functions are bounded.

3.1 First dynamical rescaling

The first rescaling is the most straight-forward one.

$$\begin{array}{lcl} w(\xi,\tau) & = & \lambda^{\alpha}(t)V(x,t), \\ \phi(\xi,\tau) & = & \lambda^{\gamma}(t)U(x,t), \\ \tau & = & \int_0^t \frac{1}{\lambda^{\beta}(s)}ds, \\ \xi & = & \frac{x}{\lambda^{\nu}(t)}, \end{array} \tag{8}$$

where $\lambda(t) \to 0$ as $t \to T$ again, and α, β, γ and ν are all positive.
So the variables and the functions U and V depend on the same function λ, but all with different powers of it. This means that it is not yet determined what the relations between the different functions and variables are. The choice of the function λ is not determined yet. In this rescaling and the others it is assumed that the pulse occurs at $x = 0$. To change this pulse position to x_0, the x in the ξ definition can be replaced by $x - x_0$. A modification like this does however does not change our analysis. In the code we used for simulations displayed later in this thesis the pulse is positioned in the middle of the x-axis. In these simulations we chose the length of this axis equal to 10, therefore the pulse lies at $x = 5$.

3.2 Second dynamical rescaling

The second rescaling was obtained from [2]. In this article blow-up in a different PDE is studied, the one component equation:

$$u_t = u_{xx} + u^\beta,$$

where $\beta > 1$. We can see that for $\beta = 2$, this equation is similar to the equations in system (1), except for the linear terms.

$$\begin{array}{lcl} w(\xi,\tau) & = & (T-t)^\alpha V(x,t) \\ \phi(\xi,\tau) & = & (T-t)^\theta U(x,t) \\ \tau & = & \int_0^t \frac{1}{(T-s)^\beta} ds \\ \xi & = & \frac{x}{(T-t)^\gamma |\log(T-t)|^\delta} \end{array} \tag{9}$$

Again, the powers α, θ, β, γ and δ are all positive.
So here, the function L described above looks like some power of $(T-t)$. Here T is again the blow-up time. Compared to the first rescaling, the biggest difference is the log-term that is added, because when λ in the first rescaling is indeed some power of $(T-t)$, the two dynamical rescalings are very much alike. The original time-variable t can be expressed in terms of τ. When $\beta = 1$ this is:

$$t = T - e^{\log|T| - \tau}$$

This means that when $t \to T$, $\tau \to \infty$. So after performing the rescaling we would like to analyze the behavior of the system for $\tau \to \infty$. The initial solutions can converge to a stationary solution as τ approaches infinity. This is the reason we study stationary solutions in this thesis.

The log-term will later on prove to be very useful because it leads the attention to other terms in the differential equation than the former rescaling.

3.3 Third dynamical rescaling

The third dynamical rescaling is a modification of the first one.

$$\begin{array}{lcl} w(\xi,\tau) & = & \lambda^\alpha(t) V(x,t) \\ \phi(\eta,\tau) & = & \lambda^\gamma(t) U(x,t) \\ \tau & = & \int_0^t \frac{1}{\lambda^\beta(s)} ds \\ \xi & = & \frac{x}{\lambda^\nu(t)} \\ \eta & = & \frac{x}{\varepsilon^\delta \lambda^\theta(t)} \end{array} \tag{10}$$

Of course, the powers of λ are all positive.
This rescaling is quite different from the former two because here it is assumed that w does not depend on the same variables as ϕ. The space variable is scaled in two ways. This is because from the simulations in [3], one can think that the U and V solutions have the same shape, only U is stretched out compared to V. Because the system studied in this thesis is coupled, this scaling does not seem very convenient, because it means that the two PDE's depend on more than one space variable. But if $g(U)$ is constant, for example, or when a solution w is known, this does not have to be a problem. Also, ξ can be expressed in terms of η.

4 The modified Gierer-Meinhardt system with $g(U) = \frac{1}{U} + a$

In this thesis we will analyze the two modified Gierer-Meinhardt systems. The first is system (1) with $f(U) = 1$ and $g(U) = \frac{1}{U} + a$.

$$\text{(11)} \qquad \begin{cases} \varepsilon^2 U_t &= U_{xx} - \varepsilon^2 \mu U + V^2 \\ V_t &= \varepsilon^2 V_{xx} - V + \left(\frac{1}{U} + a\right) V^2 \end{cases}$$

Various simulations are done using [1]. A special thanks to J.G. Blom and P.A. Zegeling for letting me using their algorithm. The analysis we perform are on an unbounded domain, no boundary conditions are involved. The simulations we perform are on a bounded domain. However, we assume that the boundaries are away far enough so that they do not influence the behavior. The simulations give rise to the analyzations we will perform in this thesis. In some cases the solutions we find show the same behavior as in the simulations.

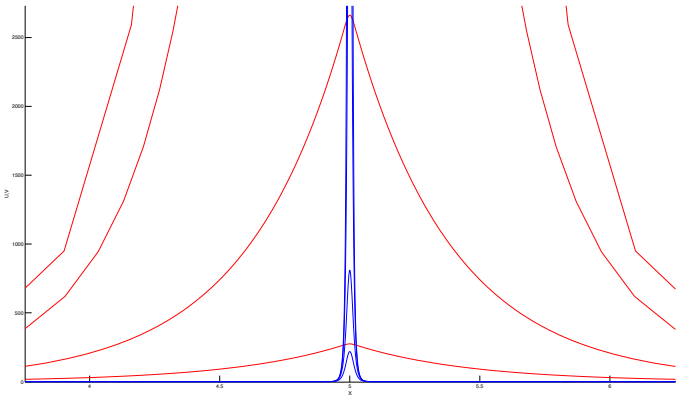

Figure 7: Simulation of (28) with $\mu = 5$, $a = 0.342$ and $\varepsilon^2 = 0.01$. The blue graphs represent V and the red graphs represent U. The solutions for $t = 10, 20, 20.5, 20.56$ are plotted. U is higher than V for all t-values. One can identify finite time blow-up. Dirichlet boundary conditions and 201 moving gridpoints are used.

For the third rescaling (as described in 3.3), it is useful to examine how the solutions change if ε varies. This way the influence of ε can be displayed.

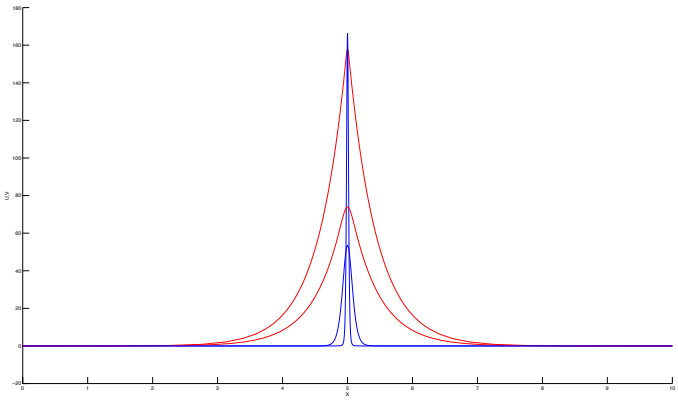

Figure 8: Simulation of (28) with $\mu = 5$ and $a = 0.342$ at $t = 5$. Again V is blue and U is red. The lowest two graphs are simulated with $\varepsilon^2 = 0.05$ and the highest two with $\varepsilon^2 = 0.01$

We find that when $\varepsilon^2 = 0.01$, for $t = 5$, the V-solution has a higher peak than U (see the largest simulations in figure 8), as in the bounded solutions simulated in [3]. For larger values of t, the solution of U apparently grows faster than V, see figure 7. When ε is larger, the graphs are smaller, and $V_{\varepsilon^2=0.05}$ is wider than $V_{\varepsilon^2=0.01}$. On the other hand is $U_{\varepsilon^2=0.05}$ narrower than $U_{\varepsilon^2=0.01}$, see figure 9. We can conclude that ε has an effect on the x-range of U and V. Also, the solutions are larger when ε is smaller. Simulations with both ε's show the same evolution in time. For small t-values, the V-pulse is higher than the U-pulse, but eventually U grows faster and U becomes larger. A difference between the simulations with the two ε's lies in the t-value where U and V are both equally large. We can see that for $t = 5$, the V solution with $\varepsilon^2 = 0.05$ is smaller than the corresponding U solution, while the V solution with $\varepsilon^2 = 0.01$ is larger than the corresponding U solution. The growth rate thus depends on ε.

4.1 The V-equation

First we will study the second equation of (11). The behavior of the V-equation has an influence on the entire system, because the system is coupled. In other words, if V blows up, the quadratic V-term in the U-equation causes blow-up for U as well. We examine:

$$V_t = \varepsilon^2 V_{xx} - V + g(U)V^2. \tag{12}$$

First we introduce the fast variable

$$z = \frac{x}{\varepsilon}.$$

In this thesis we will construct the solution to leading order. Since U becomes very large as $t \to T$, $1/U$ becomes very small. Therefore we can take $g(U) = a$ to leading order. In section 4.2.1 it is shown that this is indeed a correct assumption. Since we assume $g(U)$ to be a constant, the V equation no longer depends on U, i.e. the system is uncoupled. This yields to the following equation:

$$V_t = V_{zz} - V + aV^2. \tag{13}$$

Equation (13) will be the one analyzed in sections 4.1.1 and 4.1.2. In order to do so, we will use the first and second rescaling, which were introduced in chapter 3.1 and 3.2. Note that the rescaling introduced in 3.3 is the same as the first rescaling, if U is not incorporated in the PDE.

4.1.1 First dynamical rescaling

In this section we will obtain a solution for V using the dynamical rescaling as was discussed in paragraph 3.1. We also rescale x with ε and denote:

$$\xi = \frac{z}{\lambda^\nu(t)} = \frac{x}{\varepsilon\lambda^\nu(t)}.$$

We substitute the new variables to obtain V_t and V_{zz}.

$$\begin{aligned}
V_t &= \left[w(\xi,\tau)\lambda^{-\alpha}(t)\right]_t \\
&= \lambda^{-\alpha}\left[w(\xi,\tau)\right]_t + w\left[\lambda^{-\alpha}(t)\right]_t \\
&= \lambda^{-\alpha}\left[-z\nu\lambda^{-\nu-1}\frac{d\lambda}{dt}w_\xi + \lambda^{-\beta}w_\tau\right] + -\alpha\lambda^{-\alpha-1}\frac{d\lambda}{dt}w \\
&= -\lambda^{-\alpha-1}\frac{d\lambda}{dt}\left[z\nu\lambda^{-\nu}w_\xi + \alpha w\right] + w_\tau\lambda^{-\alpha-\beta} \\
&= w_\tau\lambda^{-\alpha-\beta} - \lambda^{-\alpha-1}\frac{d\lambda}{dt}\left[\nu\xi w_\xi + \alpha w\right] \\
V_{zz} &= \left[\frac{w(\xi,\tau)}{\lambda^\alpha}\right]_{zz} \\
&= \lambda^{-\alpha}\left[\frac{w_\xi}{\lambda^\nu} + w_\tau\cdot 0\right]_z \\
&= \lambda^{-\alpha}\lambda^{-\nu}\lambda - \nu w_{\xi\xi} \\
&= \lambda^{-2\nu-\alpha}w_{\xi\xi}
\end{aligned}$$

We can use these expressions in (13), to obtain the following equation:

$$w_\tau\lambda^{-\alpha-\beta} - \lambda^{-\alpha-1}\frac{d\lambda}{dt}\left[\nu\xi w_\xi + \alpha w\right] = \lambda^{-2\nu-\alpha}w_{\xi\xi} - \lambda^{-\alpha}w + a\lambda^{-2\alpha}w^2 \tag{14}$$

Dividing by $\lambda^{-2\nu-\alpha}$ then gives:

$$w_{\xi\xi} + \lambda^{2\nu-1}\frac{d\lambda}{dt}\left[\alpha w + \nu\xi w_\xi\right] - \lambda^{2\nu}w + a\lambda^{2\nu-\alpha}w^2 - \lambda^{2\nu-\beta}w_\tau = 0 \tag{15}$$

The difficulty in studying this equation is the time-dependence. One way to remove this inconvenience is to assume that w can be separated into two functions each depending on just one variable. For instance, if we assume that $w = e^{c\tau}Q(\xi)$, the time derivative can be expressed in terms of w itself. After that, the e-term can be divided out of the entire equation, leading to an ordinary differential equation of Q. Then the problem of time-dependence would be solved. Unfortunately, this assumption won't work in the PDE that we are studying. The problem lies in the quadratic term of w. When substituting w and then dividing by $e^{c\tau}$, one e-term remains, which still leaves a time-dependence in the equation. Therefore, this will not be a useful step.

Another way to get rid of the time-dependence is to look at stationary solutions. Setting the time derivative equal to zero, equation (15) becomes:

$$w_{\xi\xi} + \lambda^{2\nu-1}\frac{d\lambda}{dt}\left[\alpha w + \nu\xi w_\xi\right] - \lambda^{2\nu}w + a\lambda^{2\nu-\alpha}w^2 = 0. \tag{16}$$

Note that λ also depends on t. The reason these terms are not discussed as a difficulty above, is because the λ-terms are very small. Later on we will try to find

solutions to leading order of these λ's. Then some terms will be of higher order, and the ones analyzed are all of the same order. This means we can divide these terms out.

Also, notice that the $\lambda^{2\nu}w$ has a higher power of λ than $a\lambda^{2\nu-\alpha}w^2$, assuming w and w^2 are both of the same order. This means that in studying the leading order of λ in equation (16), this term will not be taken into account. This yields:

$$w_{\xi\xi} + \lambda^{2\nu-1}\frac{d\lambda}{dt}\left[\alpha w + \nu\xi w_\xi\right] + a\lambda^{2\nu-\alpha}w^2 = 0. \tag{17}$$

The ξw_ξ-term together with $\frac{d\lambda}{dt}$ can still cause some difficulties. However, note that λ can still be chosen. One choice is to assume:

$$\lambda^{2\nu-1}\frac{d\lambda}{dt} = -A,$$

where A is small enough to be of higher order than $a\lambda^{2\nu-\alpha}$. This is a differential equation which can be solved for λ using separation of variables.

$$\begin{aligned} \lambda^{2\nu-1}d\lambda &= -Adt, \\ \lambda &= \left(-2\nu A(t+c)\right)^{\frac{1}{2\nu}}, \end{aligned}$$

where c is a constant of integration. However, the claim for λ was:

$$\lim_{t\uparrow T}\lambda(t) = 0,$$

therefore we know that $c = -T$. This yields for λ:

$$\lambda(t) = \left(2\nu A(T-t)\right)^{\frac{1}{2\nu}}.$$

Substituting this in (17), gives the following equation:

$$w_{\xi\xi} - A\left[\alpha w + \nu\xi w_\xi\right] - 2\nu A(T-t)w + a(2\nu A(T-t))^{1-\frac{\alpha}{2\nu}}w^2 = 0. \tag{18}$$

We assumed that the term containing A would not be of leading order. Equation (18) can be simplified into:

$$w_{\xi\xi} + a(2\nu A(T-t))^{1-\frac{\alpha}{2\nu}}w^2 = 0. \tag{19}$$

If we want the second term to be of first order, we should choose $\alpha = 2\nu$. This way, the power of the coefficient of the quadratic term is zero, and therefore the term itself is equal to 1.

$$w_{\xi\xi} = -aw^2. \tag{20}$$

Equation (20) has solutions of the form $w = c_1\cos(\sqrt{a}\xi) + c_2\sin(\sqrt{a}\xi)$, with c_1, c_2 constants. Functions like these are definitely bounded but they do not show some sort of peak similar to the ones displayed in the numerical simulations. However, it can be that this solution can be matched to another solution. Then this could be the leading order part of the center of the pulse, and another solution will represent the decay of the pulse. It can also be due to the initial conditions of our simulations, that we do not find this cosine behavior in the numerical simulations.

However, the choices for the powers of λ we made above, can be chosen differently. This means we can determine what terms will be leading order. We go back to equation (14). The $\lambda^{-\alpha}$-term is not leading order because $\lambda^{-2\alpha}$, $\lambda - \alpha - 1$

and $\lambda^{-\alpha-\beta}$ are always larger because the powers of λ are smaller. For the leading order part of equation (14) this yields:

$$w_\tau \lambda^{-\alpha-\beta} - \lambda^{-\alpha-1}\frac{d\lambda}{dt}\left[\nu\xi w_\xi + \alpha w\right] = \lambda^{-2\nu-\alpha} w_{\xi\xi} + a\lambda^{-2\alpha} w^2. \tag{21}$$

In the former analysis the next step was to divide by the coefficient of $w_{\xi\xi}$. In doing so, we assumed that $w_{\xi\xi}$ should be of leading order but this did not lead to a solution we were looking for. A different approach to equation (21) can be to assume that the second derivative is not leading order. Therefore we must choose our α and ν in such a way that $\lambda^{-2\nu-\alpha} w_{\xi\xi}$ is of higher order than $a\lambda^{-2\alpha} w^2$. In that case, we should choose:

$$-2\nu - \alpha > -2\alpha,$$

or

$$2\nu < \alpha.$$

We will study stationary solutions, so $w_\tau = 0$. Note that this means that β can be chosen arbitrarily. The leading part of (21) is given by:

$$\lambda^{-\alpha-1}\frac{d\lambda}{dt}\left[\nu\xi w_\xi + \alpha w\right] = a\lambda^{-2\alpha} w^2. \tag{22}$$

If we want both the left- and right-hand side to be leading order terms, we should choose $\lambda^{-\alpha-1}\frac{d\lambda}{dt}$ and $\lambda^{-2\alpha}$ of the same order. This gives that:

$$\lambda^{-\alpha-1}\frac{d\lambda}{dt} = -k\lambda^{-2\alpha},$$

where k is some positive constant which is not yet determined. This leads to an expression for λ.

$$\begin{aligned} \lambda^{\alpha-1} d\lambda &= -k\lambda^{-2\alpha} dt, \\ \lambda^{\alpha} &= \alpha k(T-t), \\ \lambda(t) &= (\alpha k(T-t))^{\frac{1}{\alpha}}. \end{aligned}$$

Again, the integration constant can be determined since we know $\lim_{t\uparrow T} \lambda(t) = 0$. Substituting this expression for λ in equation (22) yields:

$$k\lambda^{-2\alpha}\left[\nu\xi w_\xi + \alpha w\right] = a\lambda^{-2\alpha} w^2.$$

Division by $\lambda^{-2\alpha}$ leads to the following ODE:

$$k\left[\nu\xi w_\xi + \alpha w\right] - aw^2 = 0, \tag{23}$$

which can be solved using separation of variables.

$$
\begin{aligned}
k\nu\xi w_\xi + k\alpha w &= aw^2, \\
k\nu\xi w_\xi &= aw^2 - k\alpha w, \\
\frac{k\nu\xi}{d\xi} &= \frac{aw^2 - k\alpha w}{dw}, \\
\frac{1}{k\nu}\int \frac{d\xi}{\xi} &= \int \frac{dw}{aw^2 - k\alpha w}, \\
\frac{1}{k\nu}(\ln|\xi| + c_1) &= \frac{a}{k\alpha}\int \frac{dw}{aw - k\alpha} - \frac{1}{k\alpha}\int \frac{dw}{w}, \\
\frac{1}{k\nu}(\ln|\xi| + c_1) &= \frac{1}{k\alpha}\ln|aw - k\alpha| - \frac{1}{k\alpha}\ln|w|, \\
\frac{\alpha}{\nu}\ln|\xi| + \frac{\alpha c_1}{\nu} &= \ln\left|\frac{aw - k\alpha}{w}\right|, \\
e^{\frac{\alpha c_1}{\nu}}\left|\xi^{\frac{\alpha}{\nu}}\right| &= \left|\frac{aw - k\alpha}{w}\right|, \\
e^{\frac{\alpha c_1}{\nu}}\xi^{\frac{\alpha}{\nu}} &= \pm\left(a - \frac{k\alpha}{w}\right).
\end{aligned}
$$

Here c_1 is an integration constant. If we define:

$$c_2 = \pm e^{\frac{\alpha}{\nu}},$$

we can rewrite the expression above into:

$$c_2\xi^{\frac{\alpha}{\nu}} = \frac{k\alpha}{w} - a.$$

Isolating w yields:

$$w = \frac{k\alpha}{a + c_2\xi^{\frac{\alpha}{\nu}}}, \tag{24}$$

where k and a are positive constants and c_2 can be either positive or negative. The shape of the solution for w depends on the constants. If c_2 is negative, we find a singularity. Therefore we choose c_2 to be positive as well. Of course, we must take into account that $2\nu < \alpha$, and if $\frac{\alpha}{\nu}$ is not an even integer the solution does not have the correct shape.
In figure 9 w is displayed for $k = a = c = 1$, $\alpha = 2$ and $\nu = \frac{1}{2}$.

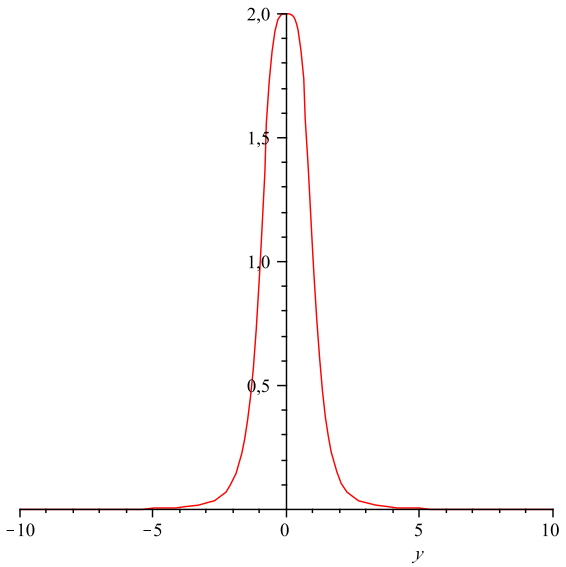

Figure 9: A plot of $w = \frac{k\alpha}{a+c_2\xi^{\frac{\alpha}{\nu}}}$ with $k = a = c = 1$, $\alpha = 2$ and $\nu = \frac{1}{2}$.

We can conclude that this solution has the shape similar to the simulations displayed in figure 7. Recall that w is the rescaled version of V such that it stays bounded. Therefore they must have approximately the same form. Up to leading order, this is a fitting solution. The reason we did not find a solution like this at first, was due to the choice we made by dividing the equation by the coefficient of the second derivative. After that, we analyzed the leading order terms, assuming that the second derivative was leading order. This, however, need not be the case.

Of course the higher order terms do have an influence on the behavior of this solution. This influence will not be discussed in this thesis.

The other constants also determine the behavior of w, see figure 10. The constants a, k and c are all chosen equal to 0.01 once. We can conclude that if k is small, the solution is compressed vertically. Horizontally nothing changes. If a is small, the pulse is larger, stretched out vertically. Finally, if c is small, the pulse is stretched out horizontally.

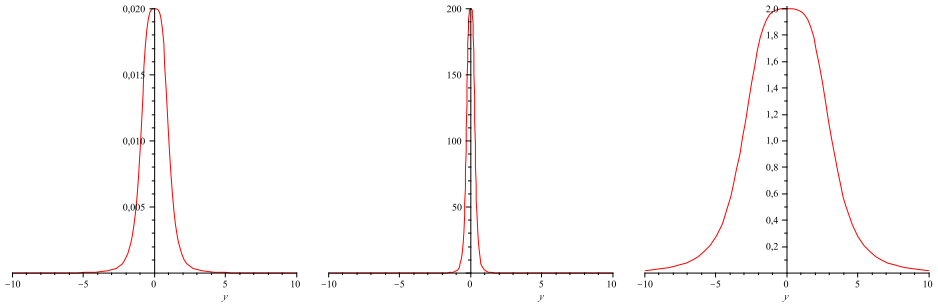

Figure 10: On the left: A plot of $w = \frac{k\alpha}{a+c_2\xi^{\frac{\alpha}{\nu}}}$ with $k = 0.01$, $a = c = 1$, $\alpha = 2$ and $\nu = \frac{1}{2}$.
In the middle: A plot of $w = \frac{k\alpha}{a+c_2\xi^{\frac{\alpha}{\nu}}}$ with $k = c = 1$, $a = 0.01$, $\alpha = 2$ and $\nu = \frac{1}{2}$.
On the right: A plot of $w = \frac{k\alpha}{a+c_2\xi^{\frac{\alpha}{\nu}}}$ with $k = a = 1$, $c = 0.01$, $\alpha = 2$ and $\nu = \frac{1}{2}$.

So using the first dynamical rescaling, we obtained an expression for the leading order part of w. Note that we only chose the powers of λ explicitly to make the plots of figures 9 and 10.

4.1.2 Second dynamical rescaling

In this section we explain why the second rescaling, introduced in section 3.2, is more convenient than the first, which differs a log-term. Explanations about this log-term and further information can be found in [2].

Again, rewrite V_t and V_{zz} in order to substitute the rescalings into the equation. We analyze the system near the blow-up time T.

$$\begin{aligned}
V_t &= \left[(T-t)^{-\alpha} w(\xi,\tau)\right]_t, \\
&= \alpha(T-t)^{-\alpha-1} w + (T-t)^{-\alpha}\left[\frac{\partial w}{\partial \xi}\frac{\partial \xi}{\partial t} + \frac{\partial w}{\partial \tau}\frac{d\tau}{dt}\right], \\
&= \alpha(T-t)^{-\alpha-1} w + (T-t)^{-\alpha} z w_\xi \left[\gamma(T-t)^{-\gamma-1}|\log(T-t)|^{-\delta}\right., \\
&- \left.\delta(T-t)^{-\gamma-1}|\log(T-t)|^{-\delta-1}\right] + w_\tau (T-t)^{-\beta-\alpha}, \\
&= \alpha(T-t)^{-\alpha-1} w + (T-t)^{-\alpha-\gamma-1}|\log(T-t)|^{-\delta} z w_\xi \left[\gamma - \frac{\delta}{|\log(T-t)|}\right] \\
&+ w_\tau (T-t)^{-\beta-\alpha}.
\end{aligned}$$

In section 3.2, ξ was defined as:

$$\xi = z(T-t)^{-\gamma}|\log(T-t)|^{-\delta},$$

therefore

$$V_t = \alpha(T-t)^{-\alpha-1} w + (T-t)^{-\alpha-1}\xi w_\xi \left[\gamma - \frac{\delta}{|\log(T-t)|}\right] + w_\tau (T-t)^{-\beta-\alpha}.$$

Also

$$V_{zz} = (T-t)^{-\alpha-2\gamma}|\log(T-t)|^{-2\delta} w_{\xi\xi}.$$

Substituting these new expressions for the derivatives of V in the original differential equation (13) we obtain:

$$\begin{aligned}
(25) \qquad &\alpha(T-t)^{-\alpha-1} w + (T-t)^{-\alpha-1}\xi w_\xi \left[\gamma - \frac{\delta}{|\log(T-t)|}\right] + w_\tau (T-t)^{-\beta-\alpha} \\
&= (T-t)^{-\alpha-2\gamma}|\log(T-t)|^{-2\delta} w_{\xi\xi} - (T-t)^{-\alpha} w + a(T-t)^{-2\alpha} w^2
\end{aligned}$$

Dividing equation (25) by $(T-t)^{-\alpha-2\gamma}$ gives:

$$\begin{aligned}
(26) \qquad &\frac{w_{\xi\xi}}{|\log(T-t)|^{2\delta}} - (T-t)^{2\gamma} w + a(T-t)^{2\gamma-\alpha} w^2 - \alpha(T-t)^{2\gamma-1} w \\
&-(T-t)^{2\gamma-1}\xi w_\xi \left[\gamma - \frac{\delta}{|\log(T-t)|}\right] + w_\tau (T-t)^{2\gamma-\beta} = 0
\end{aligned}$$

The term $(T-t)^{2\gamma}$ is very small compared to the other terms in $(T-t)$, hence this term is not of leading order, so we will not study this.

The second derivative has very small coefficient if $\delta \neq 0$, so again this is of higher order and it won't be studied. The same argumentation tells us that the other log-term in equation (26) is higher order. Note that the trivial case where $\delta = 0$ yields the first rescaling, introduced in section 3.1. If we analyze stationary solutions, the leading order part of equation (26) becomes:

$$0 = a(T-t)^{2\gamma-\alpha}w^2 - \alpha(T-t)^{2\gamma-1}w - \gamma(T-t)^{2\gamma-1}\xi w_\xi. \tag{27}$$

Thus by only taking the leading order terms into account, we have obtained a first order ordinary differential equation. We want to keep studying as many terms as possible, so we should choose the powers of λ in a way such that most terms remain in the equation at leading order. The way to do so is choosing $\alpha = 1$. Dividing equation (27) by $(T-t)^{2\gamma-1}$ yields:

$$0 = aw^2 - w - \gamma\xi w_\xi. \tag{28}$$

Notice that the leading order equation does not depend on the log-term. This means that to leading order, the two rescalings introduced in sections 3.1 and 3.2 yield the same differential equations, if $\lambda(t) = (T-t)$. Comparing equation (28) to (23), one can observe that, except for the constants, the same terms are involved. Equation (28) can be solved explicitly, analogous to the calculations on page 20.

$$w = \frac{1}{a - c_3\xi^{\frac{1}{\gamma}}}.$$

Just like before in section 4.1.1, because of the absolute value of ξ obtained by integration, we may assume that c_3 can be either positive or negative. If c_3 is negative, the expression is similar to solution (24), see figure 11.

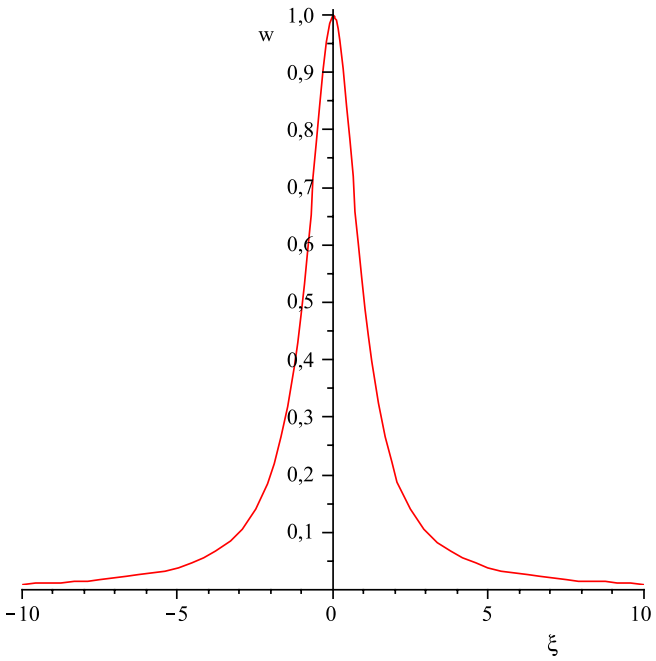

Figure 11: Plot of $w = \frac{1}{a - c_3\xi^{\frac{1}{\gamma}}}$ for $a = 1$, $\gamma = \frac{1}{2}$, and $c_3 = -1$

Even though the two rescalings used in this and the former section are different from one another, they yield the same kind of solution to leading order. We noticed before that the log-term was not involved in the leading order equation. On the other hand, in studying higher order terms this term could have a big influence. As mentioned before, the higher order terms will not be discussed in this thesis. However, the log-term was useful in the analysis of the leading order terms, because it naturally led to assuming the second derivative was small and therefore of higher order.

4.2 The coupled system

In this section we will study the entire system with its two components U and V, $f(U) = 1$ and $g(U) = \frac{1}{U} + a$:

$$\begin{cases} \varepsilon^2 U_t &= U_{xx} - \varepsilon^2 \mu U + V^2, \\ V_t &= \varepsilon^2 V_{xx} - V + \frac{V^2}{U} + aV^2. \end{cases} \tag{29}$$

We will no longer use the second rescaling as introduced in section 3.2, because the first, discussed in section 3.1, yields a similar expression to leading order but is more convenient in use. This was shown in sections 4.1.1 and 4.1.2. In this section we will use the solutions for V found in the former section in order to analyze solutions for U. First we will explain that $g = 1/U + a$ can be assumed to be constant a to leading order, as we assumed in section 4.1.1. After that we will examine the solution of V which was found in section 4.1.1 to obtain a similar solution for U, which we will compare to the simulations we performed. Finally we will use the rescaling from section 3.3 to analyze the behavior of U in another way.

4.2.1 First dynamical rescaling

We use the rescaling as was introduced in paragraph 3.1. The function U depends on the same variables x, t as V, which are rescaled into ξ and τ. Recall that we performed this rescaling in 4.1.1 for the V-component of system (29). In the same way we can rescale the U-component. First we will zoom in near the pulse, which we assumed to be at $x = 0$. Therefore we introduce the variable z:

$$z = \frac{x}{\varepsilon}.$$

Which we also introduced in section 4.1.1. System (29) becomes:

$$\begin{cases} \varepsilon^2 U_t &= \frac{1}{\varepsilon^2} U_{zz} - \varepsilon^2 \mu U + V^2, \\ V_t &= V_{zz} - V + \frac{V^2}{U} + aV^2. \end{cases} \tag{30}$$

Substituting the dynamical rescaling yields the following expressions for the derivatives of U with respect to t and z:

$$\begin{aligned} U_t &= \phi_\tau \lambda^{-\gamma-\beta} - \lambda^{-\gamma-1} \frac{d\lambda}{dt} \left[\gamma\phi + \nu\xi\phi_\xi\right], \\ U_{xx} &= \lambda^{-2\nu-\gamma} \phi_{\xi\xi}. \end{aligned}$$

The function g also alters:

$$g(U) = \frac{1}{U} + a = \lambda^\gamma \phi^{-1} + a.$$

Substituting these expressions and the ones we already obtained in section 4.1.1 into (30) gives:

$$\begin{cases} \varepsilon^2 \lambda^{-\gamma-\beta} \phi_\tau - \varepsilon^2 \lambda^{-\gamma-1} \frac{d\lambda}{dt} \left[\xi\nu\phi_\xi + \gamma\phi\right] &= \frac{1}{\varepsilon^2} \lambda^{-2\nu-\gamma} \phi_{\xi\xi} - \varepsilon^2 \mu \lambda^{-\gamma} \phi \\ & \quad + \lambda^{-2\alpha} w^2, \\ \lambda^{-\alpha-\beta} w_\tau - \lambda^{-\alpha-1} \frac{d\lambda}{dt} \left[\xi\nu w_\xi + \alpha w\right] &= \lambda^{-2\nu-\alpha} w_{\xi\xi} - \lambda^{-\alpha} w \\ & \quad + \lambda^{-2\alpha+\gamma} \phi^{-1} w^2 + a\lambda^{-2\alpha} w^2. \end{cases} \tag{31}$$

We know λ is small because we analyze the system near the pulse and near the blow-up time. Higher powers of λ are very small compared to lower powers.

Hence $\lambda^{-\alpha}$ and $\lambda^{-2\alpha+\gamma}$ are of higher order compared to $\lambda^{-2\alpha}$. Therefore these terms are not examined in the leading order part of the system (31). Comparing $\lambda^{-\gamma}$ to $\lambda^{-\gamma-1}$ leads to a similar conclusion.

In this thesis we will analyze stationary solutions up to leading order. If we assume that the time derivatives are equal to zero, the leading order part system (31) becomes:

$$\left\{ \begin{array}{lcl} -\varepsilon^2 \lambda^{-\gamma-1} \frac{d\lambda}{dt} \left[\xi\nu\phi_\xi + \gamma\phi\right] & = & \frac{1}{\varepsilon^2}\lambda^{-2\nu-\gamma}\phi_{\xi\xi} + \lambda^{-2\alpha}w^2, \\ -\lambda^{-\alpha-1} \frac{d\lambda}{dt} \left[\xi\nu w_\xi + \alpha w\right] & = & \lambda^{-2\nu-\alpha}w_{\xi\xi} + a\lambda^{-2\alpha}w^2. \end{array} \right. \tag{32}$$

Here we can see that $g(U)$ is indeed constant a to leading order. We have already found the solution for w in section 4.1.1:

$$w = \frac{k\alpha}{a + c_2 \xi^{\frac{\alpha}{\nu}}}.$$

Recall that the shape of this solution depends on the choices made for α and ν. The only assumptions we made at this point is that $2\nu < \alpha$, and $\lambda = (\alpha k(T-t))^{\frac{1}{\alpha}}$, which is the same as $\frac{d\lambda}{dt} = -k\lambda^{-\alpha+1}$.
We will examine the equation for U which is given by:

$$k\varepsilon^2 \lambda^{-\gamma-\alpha} \left[\xi\nu\phi_\xi + \gamma\phi\right] = \frac{1}{\varepsilon^2}\lambda^{-2\nu-\gamma}\phi_{\xi\xi} + \lambda^{-2\alpha}w^2. \tag{33}$$

As we mentioned before, the solution for U has a shape that is similar to the shape of V. Therefore the expressions of the solutions to leading order will be alike as well. We already assumed that $2\nu < \alpha$, therefore $\lambda^{-2\nu-\gamma}$ is smaller than $\lambda^{-\gamma-\alpha}$ and the second derivative is not leading order. Equation (33) becomes:

$$k\varepsilon^2 \lambda^{-\gamma-\alpha} \left[\xi\nu\phi_\xi + \gamma\phi\right] = \lambda^{-2\alpha}w^2. \tag{34}$$

If we would like these two terms to be both leading order terms, we should assume $\alpha = \gamma$. This does have consequences for the relation between the blow-up rate of U and V, but for now we assume that they blow up with the same rate. After multiplication by $\lambda^{2\alpha}$, the differential equation for ϕ becomes:

$$k\varepsilon^2 \left[\xi\nu\phi_\xi + \gamma\phi\right] = w^2. \tag{35}$$

A solution for w is known, therefore we can solve this ODE. First we find a homogeneous solution for equation (35).

$$\begin{array}{rcl} k\varepsilon^2 \left[\xi\nu\phi_\xi + \gamma\phi\right] & = & 0, \\ \xi\nu\frac{d\phi}{d\xi} + \gamma\phi & = & 0, \\ -\frac{\xi\nu}{\gamma d\xi} & = & \frac{\phi}{d\phi}, \\ -\frac{\gamma}{\nu}\frac{d\xi}{\xi} & = & \frac{d\phi}{\phi}, \\ \phi & = & c_4 \frac{1}{\xi^{\frac{\gamma}{\nu}}}. \end{array}$$

Next we find a particular solution for equation (35). We insert the solution for w:

$$k\varepsilon^2 \left[\xi\nu\phi_\xi + \gamma\phi\right] = \left(\frac{k\alpha}{a + c_2\xi^{\frac{\alpha}{\nu}}}\right)^2 \tag{36}$$

This equation is very similar to equation (23) we found before in section 4.1.1. Therefore we can find a similar solution for equation (36) using the solution of the former equation. We find an expression for a particular solution for ϕ:

$$\phi = \frac{1}{\varepsilon^2 a} \frac{k\alpha}{a + c_2 \xi^{\frac{\alpha}{\nu}}} = \frac{k\alpha}{\varepsilon^2 a \left(a + c_2 \xi^{\frac{\alpha}{\nu}}\right)}$$

Now we find the complete solution of equation (35):

$$\phi = c_4 \frac{1}{\xi^{\frac{\gamma}{\nu}}} + \frac{k\alpha}{\varepsilon^2 a \left(a + c_2 \xi^{\frac{\alpha}{\nu}}\right)}.$$

If c_4 is nontrivial, this solution has a singularity at $\xi = 0$. If $c_4 = 0$, ϕ is a multiplication of w. We noticed before that the simulations, see figure 4, show similar graphs for U and V. The solutions we found for w and ϕ definitely show that ϕ is larger than w, due to the fact that $\frac{1}{\varepsilon^2}$ is very large. The main difference between the expressions found and the simulations lies in the width of the pulse. In the simulations the pulse is always narrower in V than in U. This behavior is not described by the expressions we have found for w and ϕ. This could be due to several reasons. First, recall that we did zoom in at $x = 0$ and that at this level the solutions could be a multiplication of one another to leading order. We only analyzed the behavior to leading order. It could be the case that the width of the pulse is described only by higher order terms. The second derivative for example, could have a large influence in the higher order terms.

Moreover, several assumptions were made in the construction of the expressions of ϕ and w. As mentioned above the choices made for the powers of λ have consequences for the relation between ϕ and w. An assumption that could be wrongly made is the choice $\gamma = \alpha$. This means that U and V both blow up with the same rate. One can question wether this is the case. Using simulations we tried to find this out. In figure 12, a plot of U and V at two instants of time is displayed.

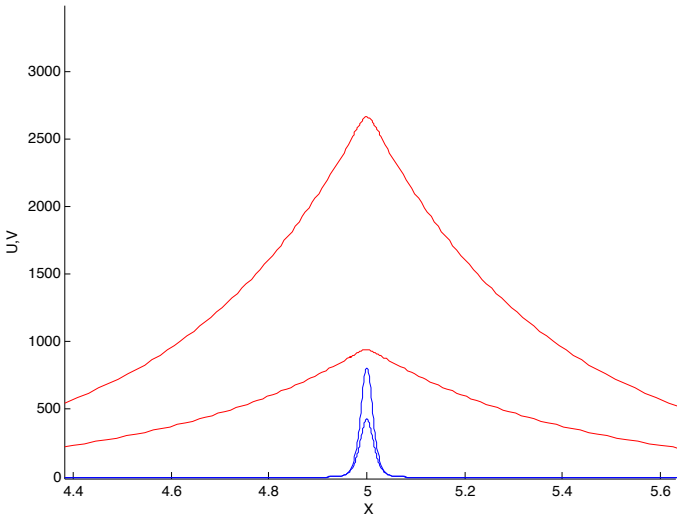

Figure 12: A plot of U and V for $\varepsilon^2 = 0.01$, $\mu = 5$ and $a = 0.342$ at $t = 19$ and $t = 20$.

The maximum of U at $t = 19$ lies at $U = 940$ and at $t = 20$ at $U = 2675$. The maximum of V at $t = 19$ lies at $V = 430$ and at $t = 20$ at $V = 800$. Thus, in

the same time-interval U has increased with a factor 2.8 and V with a factor 1.9. From this it could be deduced that the two solutions do not grow with the same rate, as was assumed in the analysis before, but that U grows faster than V. In the construction of ϕ we used that $\alpha = \gamma$, which could be a reason the difference in the width of the pulses is not described by the expressions we found for ϕ and w. However, it could also mean that the numerical simulations break down because of the extreme increase in both solutions.

Another assumption in the analysis was to take $2\nu < \alpha$, which implies that $\frac{1}{\varepsilon^2}\lambda^{-2\nu+1}\phi_{\xi\xi}$ is a higher order term. As a result of this we did not incorporate this second derivative in the analysis. What we did not discuss was the $\frac{1}{\varepsilon^2}$ coefficient. Since ε is very small, this is very large. The reason why we did not mention this earlier is that $\lambda \to 0$ for $t \to \infty$, and $\frac{1}{\varepsilon}$ is always bounded. This means that there always exists a $\tilde{t}$ such that for every $t > \tilde{t}$, $\frac{1}{\varepsilon}\lambda(t)$ gets very small and not of leading order. But in fact it could be that the ε is of importance in the leading order solution.

As we can see, there are several possibilities one could think of to be the source of the difference between the expressions found and the simulations of ϕ and w displayed in figure 4. One thing that could lead to a better fitting solution for ϕ is assuming that $\gamma > \alpha$. In that case, $\lambda^{-\gamma-\alpha}$ is larger than $\lambda^{-2\alpha}$. This means that the w-term in the ϕ-equation vanishes from equation (34). The equation then becomes:

$$\varepsilon^2 k\left[\gamma\phi + \xi\nu\phi_\xi\right] = 0$$

Which is the equation we already solved in order to find the homogeneous solution of equation (35). The solution was:

$$\phi = \frac{c_4}{\xi^{\frac{\gamma}{\nu}}}.$$

This solution has a singularity at $\xi = 0$, however, we require it to stay bounded.

We can also assume that $\gamma > \alpha$, and in addition assume that in equation (33) the second derivative term is of the same order as $\varepsilon^2\lambda^{-\gamma-\alpha}$. The ϕ-equation looks like:

$$k\left[\gamma\phi + \xi\nu\phi_\xi\right] = \phi_{\xi\xi}, \tag{37}$$

which can be rewritten into a parabolic cylinder equation. Therefore we first introduce a new variable ζ which is given by:

$$\zeta = \sqrt{k\gamma}\xi.$$

Substituting this into equation (37) yields:

$$\phi_{\zeta\zeta} - \phi - \frac{\nu}{\gamma}\zeta\phi_\zeta = 0. \tag{38}$$

Now we assume that the function ϕ can be expressed as a multiplication of two functions, say:

$$\phi = X(\zeta)W(\zeta).$$

Substituting this into equation (38) gives the following differential equation for W:

$$XW_{\zeta\zeta} + \left(2X_\zeta - \frac{\nu}{\gamma}\zeta X\right)W_\zeta + \left(X_{\zeta\zeta} - X - \frac{\nu}{\gamma}\zeta X_\zeta\right)W = 0. \tag{39}$$

Now we assume that the coefficient of the first derivative of W is equal to zero, i.e., that the equation for W is self-adjoint. We can obtain an expression for X:

$$\begin{aligned} 2X_\zeta - \frac{\nu}{\gamma}\zeta X &= 0, \\ X(\zeta) &= c_5 e^{\frac{\nu}{4\gamma}\zeta^2}. \end{aligned}$$

We can substitute this expression into equation (39) to yield a differential equation for W. Because X is an exponential function, its derivatives with respect to ζ are all in terms of the function itself. After dividing these terms out we find:

$$W_{\zeta\zeta} + W\left(\frac{3\nu^2}{4\gamma^2}\zeta^2 - \frac{\nu}{2\gamma} - 1\right) = 0. \tag{40}$$

Next we perform another rescaling and introduce the variable χ

$$\chi = \frac{\zeta}{c},$$

where c is a constant we will determine later. Substituting z in equation (40) gives:

$$\frac{1}{c^2}W_{\chi\chi} + W\left(\frac{3\nu^2c^2}{4\gamma^2}\chi^2 + \frac{\nu}{2\gamma} - 1\right) = 0. \tag{41}$$

Equation (41) can be simplified:

$$W_{\xi\xi} + \frac{3\nu c^4}{\gamma^2}W\left(\frac{1}{4}\chi^2 - \frac{\gamma(\nu+3\gamma)}{6\nu^2c^2}\right) = 0.$$

Assuming $\frac{3\nu c^4}{\gamma^2} = -1$, yields $c^4 = \frac{-\gamma^2}{3\nu^2}$. This gives us a standard parabolic cylinder function. For $\nu = 1/2$ and $\gamma = 4$ the function becomes:

$$W_{\xi\xi} - W\left(\frac{1}{4}\chi^2 + \frac{10}{3}\sqrt{3}i\right) = 0. \tag{42}$$

This is a second order equation and therefore it has solutions consisting of linear combinations of two distinct solutions. The expression for $X(\zeta)$ has now become:

$$X(\chi) = c_5 e^{\frac{1}{4\sqrt{3}}i\chi^2}.$$

This means that:

$$\phi = c_5 e^{\frac{1}{4\sqrt{3}}i\chi^2} W.$$

One choice of a linear combination of solutions for W yields the plot displayed in figure 13. What we see is not exactly what we found in the numerical simulations. However, it does show a pulse. Different linear combination can modify this pulse. The center part of this pulse can be matched to a different solution with can yield a solution that does have the same shape as was simulated. This interesting case needs some further research.

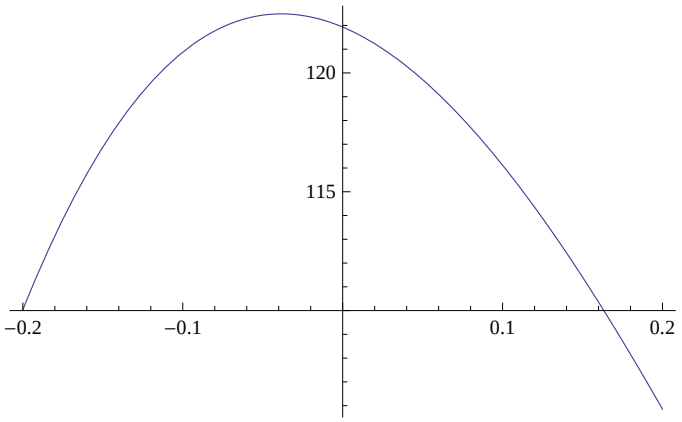

Figure 13: A plot of ϕ for a certain linear combination of solutions of W.

4.2.2 Third dynamical rescaling

In this section we will study the coupled system with respect to the third dynamical rescaling as was introduced in section 3.3. As one can see in chapter 3, the first and third rescaling are completely the same for V, because w depends on the same variables. The g-function we are examining in this chapter is constant a to leading order and therefore it does not depend on ϕ. This means that the w-equation does not depend on ϕ. If ϕ was included in the w-equation, the rescaling from section 3.3 would not be very convenient in use because the w-equation would depend on two different space variables. Since this is not the case, and we already found a solution for w, we can use this rescaling without any trouble caused by the two different x-rescalings for w and ϕ. In the former section we found an expression for ϕ that did not exactly match the simulations displayed in figure 4. The difference lies in the width of the pulse. In this rescaling, the functions U and V depend on different space variables. Not only is the ε involved in the scaling, the two variables can depend on λ with different rates as well. We would like the spatial variable corresponding to ϕ to be wider than the spatial variable corresponding to w. The difference in range of the spatial variables lies in the choices for δ and θ. We must choose $\delta > 1$ and/or $\theta > \nu$ to obtain that the spatial variable of ϕ is of a wider range than the spatial variable of w.

We already found a solution for w in the former section and for now we assume that w is given by that solution, hence,

$$w = \frac{k\alpha}{a + c_2 \xi^{\frac{\alpha}{\nu}}}.$$

In figures 9 and 10 we have also seen that for suitable α and ν this is indeed a pulse-like solution. The choices that were made to construct this solution were $2\nu < \alpha$ and $\lambda(t) = (\alpha k(T-t))^{\frac{1}{\alpha}}$. We will take these assumptions into account when we are constructing a solution for U.

First we rescale the U-equation of system (11) using the rescaling in section 3.3.

$$\begin{aligned} U_t &= \left[\phi\lambda^{-\gamma}\right]_t, \\ &= \phi\left[\lambda^{-\gamma}(t)\right] + \phi_t\lambda^{-\gamma}(t), \\ &= \phi\left[-\gamma\lambda^{-\gamma-1}\frac{d\lambda}{dt}\right] + \lambda^{-\gamma}\left[\phi_\tau\frac{d\tau}{dt} + \phi_\eta\frac{d\eta}{dt}\right], \\ &= -\gamma\lambda^{-\gamma-1}\frac{d\lambda}{dt}\phi + \lambda^{\beta-\gamma}\phi_\tau - \theta\phi_\eta\varepsilon^{-\delta}x\lambda^{-\theta-1}\frac{d\lambda}{dt}\lambda^{-\gamma}, \\ &= \lambda^{-\gamma-1}\frac{d\lambda}{dt}\left[-\gamma\phi - \theta\eta\phi_\eta\right] + \lambda^{-\beta-\gamma}\phi_\tau. \end{aligned}$$

$$\begin{aligned} U_{xx} &= \left[\phi\lambda^{-\gamma}\right]_{xx}, \\ &= \lambda^{-\gamma-2\theta}\varepsilon^{-2\delta}\phi_{\eta\eta}. \end{aligned}$$

For the U-equation this then gives:

$$\begin{aligned} \varepsilon^2\left(\lambda^{-\gamma-1}\frac{d\lambda}{dt}\left[-\gamma\phi - \theta\eta\phi_\eta\right] + \lambda^{-\beta-\gamma}\phi_\tau\right) &= \lambda^{-\gamma-2\theta}\varepsilon^{-2\delta}\phi_{\eta\eta} \\ &- \varepsilon^2\mu\lambda^{-\gamma}\phi + \lambda^{-2\alpha}w^2. \end{aligned}$$

We substitute the assumptions we made during the construction of the w solution. This yields:

$$\begin{aligned} \varepsilon^2\left(k\lambda^{-\gamma-\alpha}\left[\gamma\phi + \theta\eta\phi_\eta\right] + \lambda^{-\gamma-\beta}\phi_\tau\right) &= \lambda^{-\gamma-2\theta}\varepsilon^{-2\delta}\phi_{\eta\eta} \\ &- \varepsilon^2\mu\lambda^{-\gamma}\phi + \lambda^{-2\alpha}w^2. \end{aligned}$$

Note that the term $\varepsilon^2\lambda^{-\gamma}$ is higher order compared to the first term in the equation. We will focus on stationary solutions again, so assume $\phi_\tau = 0$.

$$k\varepsilon^2\lambda^{-\gamma-\alpha}\left[\theta\eta\phi_\eta + \gamma\phi\right] = \varepsilon^{-2\delta}\lambda^{-\gamma-2\theta}\phi_{\eta\eta} + \lambda^{-2\alpha}w^2, \tag{43}$$

where

$$w = \frac{k\alpha}{a + c_2\xi^{\frac{\alpha}{\nu}}}.$$

Expressing the various spatial variables into each other gives:

$$\xi = \frac{z}{\lambda^\nu(t)} = \frac{x}{\varepsilon\lambda^\nu} = \eta\varepsilon^{\delta-1}\lambda^{\theta-\nu}.$$

We find w in terms of η:

$$\frac{k\alpha}{a + c_2\eta^{\frac{\alpha}{\nu}}\varepsilon^{\frac{\alpha\delta-\alpha}{\nu}}\lambda^{\frac{\alpha\theta-\alpha\nu}{\nu}}}$$

Recall that δ and θ should be chosen such that $\delta > 1$ and/or $\theta > \nu$. Also, we found in the simulations that $\gamma > \alpha$ because U grows with a faster rate than V. Therefore $\lambda^{-2\alpha}$ is always higher order compared to $\lambda^{-\gamma-\alpha}$. The constant θ can be chosen in such a way that both $\lambda^{-\gamma-\alpha}$ and $\lambda^{-\gamma-2\theta}$ are leading order terms, i.e. $\alpha = 2\theta$. Dividing equation (43) by $\lambda^{-\gamma-\alpha}$ yields:

$$k\varepsilon^2 \left[\theta\eta\phi_\eta + \gamma\phi\right] = \varepsilon^{-2\delta}\phi_{\eta\eta}, \tag{44}$$

which can be rewritten into a parabolic cylinder function, like in section 4.2.1. If $\theta > \nu$, the expression for w will depend on λ. If we assume that this term is of higher order, w would just be a constant to leading order.

Another choice can be $\theta = \nu$. If $\delta > 1$, we still find that the spatial variable of ϕ is of a wider range than the spatial variable of w. We obtain an expression for w which no longer depends on λ:

$$w = \frac{k\alpha}{a + c_2\eta^{\frac{\alpha}{\nu}}\varepsilon^{\frac{\alpha\delta-\alpha}{\nu}}}.$$

Also, we could assume that $\gamma = \alpha$. We already found in the simulations that this might not be the case, but in the numerical simulations we cannot examine the behavior very close to the blow-up time, so maybe near the blow-up time the blow-up rate is the same.

The assumptions we made give us that $\lambda^{-\gamma-2\theta}$ is a higher order term compared to $\lambda^{-\gamma-\alpha} = \lambda^{-2\alpha}$. After division by $\lambda^{-2\alpha}$ the leading order part of the ODE for ϕ which was described in equation (43) becomes:

$$k\varepsilon^2 \left[\theta\eta\phi_\eta + \gamma\phi\right] = \left(\frac{k\alpha}{a + c_2\eta^{\frac{\alpha}{\nu}}\varepsilon^{\frac{\alpha\delta-\alpha}{\nu}}}\right)^2, \tag{45}$$

We can solve this equation by variation of constants. Therefore we first construct a solution for the homogeneous equation.

$$k\varepsilon^2 \left[\theta\eta\phi_\eta + \gamma\phi\right] = 0.$$

This was already discussed in 4.2.1 on page 26, and has solution:

$$\phi = \frac{G}{\eta^{\frac{\gamma}{\theta}}}$$

Where G is a constant. Now assume that G is a function of η. Substitute $\phi = \frac{G(\eta)}{\eta^{\frac{\gamma}{\theta}}}$ into (45),

$$\begin{aligned}
k\varepsilon^2 \left[\theta\eta\phi_\eta + \gamma\phi\right] &= \left(\frac{k\alpha}{a + c_2\eta^{\frac{\alpha}{\nu}}\varepsilon^{\frac{\alpha\delta-\alpha}{\nu}}}\right)^2, \\
k\varepsilon^2 k\left[\theta\eta\left(\frac{G'(\eta)}{\eta^{\frac{\gamma}{\theta}}} - \frac{\gamma}{\theta}\frac{G(\eta)}{\eta^{\frac{\gamma}{\theta}+1}}\right) + \frac{\gamma G'(\eta)}{\eta^{\frac{\gamma}{\theta}}}\right] &= \left(\frac{k\alpha}{a + c_2\eta^{\frac{\alpha}{\nu}}\varepsilon^{\frac{\alpha\delta-\alpha}{\nu}}}\right)^2, \\
\frac{k\varepsilon^2\theta G'(\eta)}{\eta^{\frac{\gamma}{\theta}-1}} &= \left(\frac{k\alpha}{a + c_2\eta^{\frac{\alpha}{\nu}}\varepsilon^{\frac{\alpha\delta-\alpha}{\nu}}}\right)^2, \\
G'(\eta) &= \frac{\eta^{\frac{\gamma}{\theta}-1}}{k\varepsilon^2\theta}\left(\frac{k\alpha}{a + c_2\eta^{\frac{\alpha}{\nu}}\varepsilon^{\frac{\alpha\delta-\alpha}{\nu}}}\right)^2, \\
G(\eta) &= \int \frac{\eta^{\frac{\gamma}{\theta}-1}}{k\varepsilon^2\theta}\frac{k^2\alpha^2}{\left(a + c_2\eta^{\frac{\alpha}{\nu}}\varepsilon^{\frac{\alpha\delta-\alpha}{\nu}}\right)^2}d\eta, \\
G(\eta) &= c_6 - \frac{\alpha^2 k}{c_2\varepsilon^{\frac{\alpha\delta-\alpha}{\nu}+2}\left(a + c_2\eta^{\frac{\alpha}{\nu}}\varepsilon^{\frac{\alpha\delta-\alpha}{\nu}}\right)}.
\end{aligned}$$

Note that $\frac{\gamma}{\theta} = \frac{\alpha}{\nu}$. This gives the solution for ϕ:

$$\phi = \frac{G(\eta)}{\eta^{\frac{\gamma}{\theta}}} = \frac{1}{\eta^{\frac{\gamma}{\theta}}} \left(c_6 - \frac{\alpha^2 k}{c_2 \varepsilon^{\frac{\alpha\delta-\alpha}{\nu}+2} \left(a + c_2 \eta^{\frac{\alpha}{\nu}} \varepsilon^{\frac{\alpha\delta-\alpha}{\nu}} \right)} \right) \tag{46}$$

This solution has a singularity at $\eta = 0$, and since we would like to find a solution that stays bounded, this does not match our requirements.

5 The modified Gierer-Meinhardt system with $g(U) = \frac{1}{U} + \frac{b}{\sqrt{U}}$

Another modified Gierer-Meinhardt system is the one where $g(U) = \frac{1}{U} + \frac{b}{U}$ and $f(U) = 1$. First we examined this system by performing numerical simulations. This was not an easy task because in some cases we encountered the limitations of the simulation of blow-up solutions. The plots do not differ very much from the simulations of the other modified Gierer-Meinhardt. Again, we find that the peak of U is larger than the peak of V and that U blows up faster, see figure 14 where plots of equidistant time-steps are given.

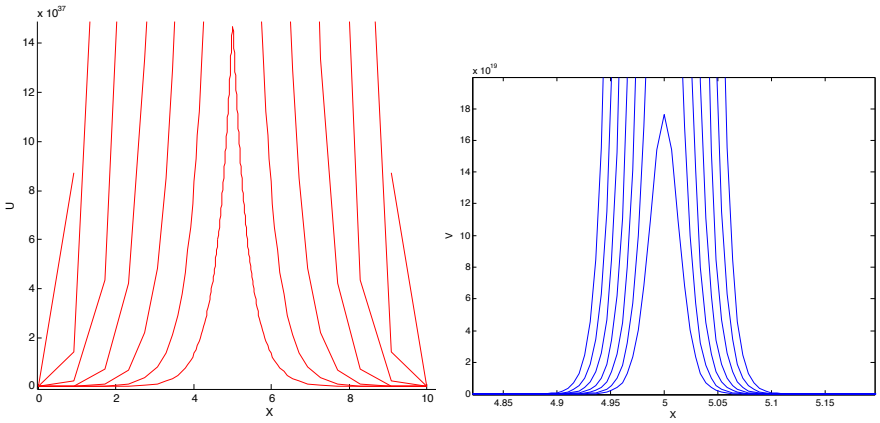

Figure 14: Simulation of U(left, red) and V(right, blue) with $b = 1.5, \varepsilon = 0.1$ and $\mu = 5$ at times $t = 90, 92, 94, 96, 98, 100, 102$, the simulations cannot be performed for $t > 102$. 201 moving grid points and Dirichlet boundary conditions were used.

So with this g-function the solutions also blow-up in finite time for various choices of μ and b. The main difference with the simulations in the former chapter is that U is many factors larger than V, see the orders of the scale of the U- and V-axis in figure 14. We cannot determine the blow-up time correctly because we encounter the limitations of the simulation of blow-up solutions. The solutions increase too much to perform the simulations. It seems obvious that when the solutions are of $\mathcal{O}(10^{37})$, we can assume that this means blow-up behavior, but the exact time when this happens is not clear because due to the largeness of the solutions they cannot be displayed correctly.

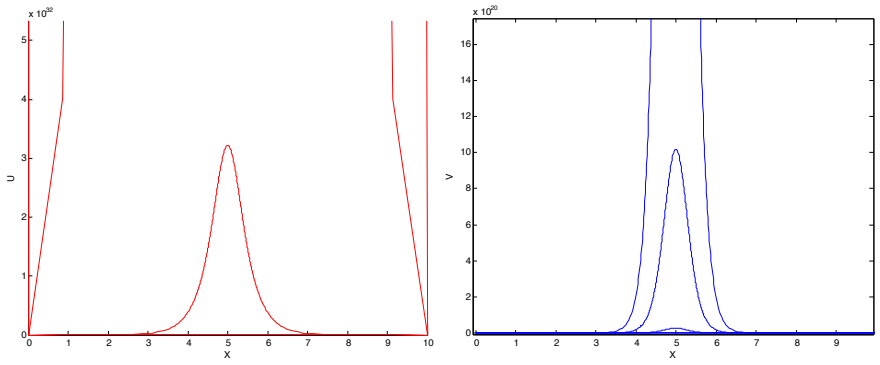

Figure 15: Simulation of U(left, red) and V(right, blue) with $b = 1.5, \varepsilon = 0.5$ and $\mu = 5$ at times $t = 20, 30, 35, 40$, the simulations cannot be performed for $t > 40$. 201 moving grid points and Dirichlet boundary conditions were used.

In figure 15 the magnitude of ε is increased. We find that for larger values of ε the solutions blow up faster. We cannot examine the difference in width of the pulse for different values of ε. What we do observe is that for both ε's the solutions have a similar shape.

Another aspect we look at is the rate of the blow-up of U and V. We do this in a similar way as in the previous section.

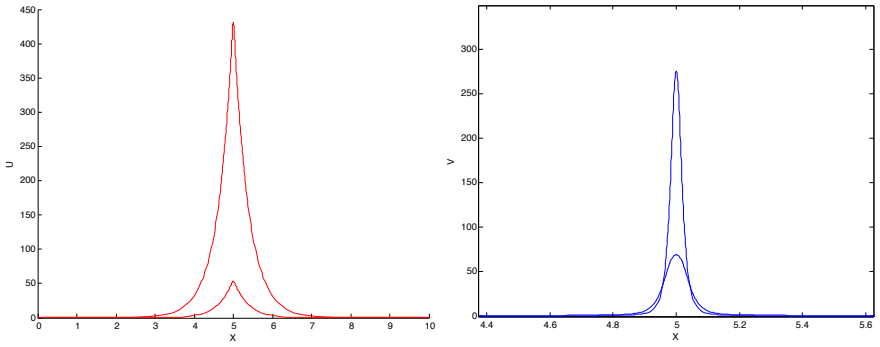

Figure 16: Simulation of U and V with $\varepsilon = 0.1$, $b = 1.5$ and $\mu = 5$ for $t = 1, 2$. 201 moving gridpoints and Dirichlet boundary conditions were used.

The U solutions has its maximum at $U = 55$ for $t = 1$ and at $U = 430$ for $t = 2$. This is a multiplication by a factor 7.8. The V solution has its maximum at $V = 75$ for $t = 1$ and $V = 275$ for $t = 2$, which is a multiplication by 3.7. Hence, we conclude that there is a difference in blow-up rate. As discussed in section 3, we study stationary solutions and this can be a solution for $t \to T$, i.e. near the blow-up time. We cannot examine the blow-up rate near the blow-up time due to the limitations of the simulation software.

Next we will consider the first rescaling to analyze the system:

$$\left\{ \begin{array}{lcl} \varepsilon^2 U_t & = & U_{xx} - \varepsilon^2 \mu U + V^2, \\ V_t & = & \varepsilon^2 V_{xx} - V + g(U) V^2, \end{array} \right. \tag{47}$$

where $g = \frac{1}{U} + \frac{b}{\sqrt{U}}$. After the rescaling we also did in 4.2.1, we find the following system:

$$(48)\quad \begin{cases} \varepsilon^2\lambda^{-\gamma-\beta}\phi_\tau - \varepsilon^2\lambda^{-\gamma-1}\frac{d\lambda}{dt}\left[\xi\nu\phi_\xi + \gamma\phi\right] &= \frac{1}{\varepsilon^2}\lambda^{-2\nu-\gamma}\phi_{\xi\xi} - \varepsilon^2\mu\lambda^{-\gamma}\phi \\ & \quad +f(U)\lambda^{-2\alpha}w^2, \\ \lambda^{-\alpha-\beta}w_\tau - \lambda^{-\alpha-1}\frac{d\lambda}{dt}\left[\xi\nu w_\xi + \alpha w\right] &= \lambda^{-2\nu-\alpha}w_{\xi\xi} - \lambda^{-\alpha}w \\ & \quad +g(U)\lambda^{-2\alpha}w^2. \end{cases}$$

Incorporating the rescaling $U = \lambda^{-\gamma}\phi$, this gives:

$$g(U) = \lambda^{\gamma}\phi^{-1} + b\lambda^{\frac{1}{2}\gamma}\phi^{-\frac{1}{2}}.$$

Substituting the rescaling then leads to:

$$(49)\quad \begin{cases} \varepsilon^2\lambda^{-\gamma-\beta}\phi_\tau - \varepsilon^2\lambda^{-\gamma-1}\frac{d\lambda}{dt}\left[\xi\nu\phi_\xi + \gamma\phi\right] &= \frac{1}{\varepsilon^2}\lambda^{-2\nu-\gamma}\phi_{\xi\xi} - \varepsilon^2\mu\lambda^{-\gamma}\phi \\ & \quad + \lambda^{-2\alpha}w^2, \\ \lambda^{-\alpha-\beta}w_\tau - \lambda^{-\alpha-1}\frac{d\lambda}{dt}\left[\xi\nu w_\xi + \alpha w\right] &= \lambda^{-2\nu-\alpha}w_{\xi\xi} - \lambda^{-\alpha}w \\ & \quad + \lambda^{-2\alpha}w^2\left(\lambda^{\gamma}\phi^{-1} + b\lambda^{\frac{1}{2}\gamma}\phi^{-\frac{1}{2}}\right). \end{cases}$$

We will look at stationary solutions again, so we set the time derivatives equal to zero.

Then, $\lambda^{-\alpha}$, $\lambda^{-\gamma}$ and $\lambda^{-2\alpha+\gamma}$ are higher order compared to $\lambda^{-\alpha-1}$, $\lambda^{-\gamma-1}$ and $\lambda^{-2\alpha+\frac{1}{2}\gamma}$ respectively. We study the leading order equations given by:

$$(50)\quad \begin{cases} -\varepsilon^2\lambda^{-\gamma-1}\frac{d\lambda}{dt}\left[\xi\nu\phi_\xi + \gamma\phi\right] &= \frac{1}{\varepsilon^2}\lambda^{-2\nu-\gamma}\phi_{\xi\xi} + \lambda^{-2\alpha}w^2, \\ -\lambda^{-\alpha-1}\frac{d\lambda}{dt}\left[\xi\nu w_\xi + \alpha w\right] &= \lambda^{-2\nu-\alpha}w_{\xi\xi} + b\lambda^{-2\alpha+\frac{1}{2}\gamma}\phi^{-\frac{1}{2}}w^2. \end{cases}$$

Note that the system becomes much more involved for $g(U) = \frac{1}{U} + \frac{b}{\sqrt{U}}$: the w-equation is now depends on ϕ. This means that we cannot use the methods that we applied for the previous choice of g. In the second chapter we already found some expressions for U and V at different levels. We can substitute these expressions into ϕ and w and find out wether they are solutions of the system to leading order.

First we will consider the ϕ-equation

$$(51)\qquad -\varepsilon^2\lambda^{-\gamma-1}\frac{d\lambda}{dt}\left[\xi\nu\phi_\xi + \gamma\phi\right] = \frac{1}{\varepsilon^2}\lambda^{-2\nu-\gamma}\phi_{\xi\xi} + \lambda^{-2\alpha}w^2.$$

The blow-up rate of U is larger than the blow-up rate of V, therefore we assume $\gamma > \alpha$. We can construct a ϕ-solution which is approximately constant near $\xi = 0$. The reason why we search for a constant ϕ-solution is because a constant was found in chapter 2. Near $\xi = 0$, the $\xi\phi_\xi$-term is very small because ξ is near 0. Assume that $\lambda^{-\gamma-1}\frac{d\lambda}{dt}$, $\lambda^{-2\nu-\gamma}$ and $\lambda^{-2\alpha}$ are all leading order. Also, we can assume that $w(\xi)$ is a constant function w_0 near ξ. Then equation (51) becomes:

$$(52)\qquad -\varepsilon^2\left[\xi\nu\phi_\xi + \gamma\phi\right] = \frac{1}{\varepsilon^2}\phi_{\xi\xi} + w_0^2.$$

Which has solutions of the form:

$$\phi(\xi) = a_1\sin\left(\sqrt{\gamma}\varepsilon^2\xi\right) + a_2\cos\left(\sqrt{\gamma}\varepsilon^2\xi\right) - \frac{w_0}{\gamma\,\varepsilon^2},$$

and if $a_1 = 0$ and $a_2 > \frac{w_0}{\gamma\,\varepsilon^2}$, this is a positive solution near $\xi = 0$. Since ε^2 is very small, the cosine will be approximately constant, and therefore the ϕ-solution will be approximately constant near $\xi = 0$.

So now we assume that ϕ is a constant that we name ϕ_0 and study the w-equation.

$$-\lambda^{-\alpha-1}\frac{d\lambda}{dt}\left[\xi\nu w_\xi+\alpha w\right]=\lambda^{-2\nu-\alpha}w_{\xi\xi}+b\lambda^{-2\alpha+\frac{1}{2}\gamma}\phi_0^{-\frac{1}{2}}w^2 \tag{53}$$

This is an equation that is similar to equation (21) with $w_\tau=0$ and $a=b\phi_0^{-\frac{1}{2}}$. In a similar way as we used in section 4.1.1 we can find a pulse-like solution for w. So near $\xi=0$ the behavior of ϕ and w could be constant for ϕ and pulse-like for w. This is consistent with the behavior found in the simulations, near the pulse.

Next we construct a solution far from the pulse. First we zoom out by substituting:

$$y=\varepsilon\xi$$

This only alters the derivatives of (50). Substitution leads to:

$$\left\{\begin{array}{lcl}-\varepsilon^2\lambda^{-\gamma-1}\frac{d\lambda}{dt}\left[y\nu\phi_y+\gamma\phi\right] & = & \lambda^{-2\nu-\gamma}\phi_{yy}+\lambda^{-2\alpha}w^2\\ -\lambda^{-\alpha-1}\frac{d\lambda}{dt}\left[y\nu w_y+\alpha w\right] & = & \varepsilon^2\lambda^{-2\nu-\alpha}w_{yy}+b\lambda^{-2\alpha+\frac{1}{2}\gamma}\phi^{-\frac{1}{2}}w^2\end{array}\right. \tag{54}$$

Next we will examine wether $w=0$ and $\phi=e^{-my}$ are solutions for some positive m. These functions are found in chapter 2. The solutions $w=0$ indeed satisfies the w-equation. Now consider:

$$-\varepsilon^2\lambda^{-\gamma-1}\frac{d\lambda}{dt}\left[y\nu\phi_y+\gamma\phi\right]=\lambda^{-2\nu-\gamma}\phi_{yy}+\lambda^{-2\alpha}w^2$$

Substitute $w=0$ and $\phi=e^{-my}$:

$$\varepsilon^2\lambda^{-\gamma-1}\frac{d\lambda}{dt}\left[-y\nu me^{-my}+\gamma e^{-my}\right]=m^2\lambda^{-2\nu-\gamma}e^{-my}$$

Assume that $\lambda^{-\gamma-1}\frac{d\lambda}{dt}=h\left(\lambda^{-2\nu-\gamma}\right)$, ($h$ a constant), and divide by $m^2\lambda^{-2\nu-\gamma}e^{-my}$:

$$\frac{\varepsilon^2}{m^2}h\left[-y\nu m+\gamma\right]=1.$$

If we choose $m=\varepsilon$ we obtain:

$$h\left[-y\nu\varepsilon+\gamma\right]=1.$$

Since ε is very small, this is correct to leading order if $h=\frac{1}{\gamma}$. Note that the behavior is now described for $y\ll\frac{1}{\varepsilon}$, and not for $y\to\infty$. Then the solutions $\phi=0$ and $w=0$ solve the system. So the behavior far from the pulse is also consistent with the simulations.

6 Conclusions

In this thesis we analyzed two modified Gierer-Meinhardt systems contained in class (1). This is a class of coupled reaction diffusion systems. In both these systems blow-up behavior was simulated. In order to examine this behavior we first did a short analysis of the bounded solutions. Next we introduced three different dynamical rescalings, which are necessary in the analysis of blow-up solutions. First we examined a a modified Gierer-Meinhardt system with $g(U) = \frac{1}{U} + a$. Since U blows up, this becomes constant to leading order. Therefore the second equation of the system does not depend on U and the system can be uncoupled. We constructed several solutions for the rescaled version of V. We also performed a lot of simulations of the system and compared the solutions to these simulations. What was found is that the leading order solutions we constructed did describe the shape of the functions that were also displayed in the simulations. This is for both U and V a pulse-like solution. On the other hand, the solutions did not describe the difference in width of the pulse. This is mainly due to the fact that we have constructed solutions of leading order.

In order to find a solution that did describe the difference in the width of the two pulses for U and V, we used different dynamical rescalings. We found several solutions. Among them was a parabolic cylinder function. This needs some further research to see wether this matches our simulations. It is possible that this solution is partially correct to leading order. The solution can show the pulse that was found in the simulations for example, even though it does not describe the correct behavior away from the pulse.

We also examined the Gierer-Meinhardt system for $g(U) = \frac{1}{U} + \frac{b}{\sqrt{U}}$. In the analysis of blow-up behavior in this system we encountered some difficulties. First, several simulations we performed could not be displayed correctly because of their magnitude. Second, this g-function is not constant to leading order. Therefore the system cannot be uncoupled and it is difficult to find solutions, because both equations depend on both functions U and V. Next we matched the solutions found in the first analysis of the bounded solutions with this system. In order to do so we studied the system in several spatial scales. Here we found that there are indeed similar solutions for this modified Gierer-Meinhardt system. This is also found in the simulations of the bounded system and the blow-up simulations. Both show that U and V both have a pulse and that the width of the pulse of U is wider than the width of the pulse of V.

7 Acknowledgements

I would like to thank my supervisor Vivi Rottschäfer for her numerous instructions and endless patience. Without her support and accompaniment I could never have written this thesis. Aside from this article she taught me a lot about examining blow-up and reaction-diffusion systems in general.
I would also like to thank Frits Veerman for his help in the search for background-information about the Gierer-Meinhardt system and his help with chapter 2.

References

[1] J.G. Blom and P.A. Zegeling, *Algorithm* 731: *A moving-grid interface for systems of one-dimensional time-dependent partial differential equations*, ACM Trans. Math. Software, 20 (1994), pp. 194-214.

[2] C.J. Budd, G.J. Collins and V.A. Galaktionov, *An asymptotic and numerical description of self-similar blow-up in quasilinear parabolic equations*, Journal of Computational and Applied Mathematics, 97 (1998), pp. 51-80.

[3] A. Doelman and T.J. Kaper, *Semistrong Pulse Interactions in a Class of Coupled Reaction-Diffusion Equations*, SIAM J. Applied Dynamical Systems, 2 (2003), pp. 53-96

[4] A. Gierer and H. Meinhardt, *A theory of biological pattern formation*, Kybernetic, 12 (1972), pp. 1087-1097.

[5] A.J. Koch and H. Meinhardt, *Biological pattern formation: from basic mechanisms to complex structures*, Reviews of Modern Physics, 66 (1994), pp. 1481-1500.